

## AN ABSTRACT OF THE THESIS OF

Junwei Jia for the degree of Master of Science in Radiation Health Physics presented on March 13, 2017.

Title: Beehive Model Creation for Use in Determining Radiation Dose to Beeswax and Bee Larvae.

Abstract approved:

---

Kathryn A. Higley

Honeybees and honey combs are good indicators of environmental contamination and can be important for dose calculations. In the event of reactor accidents and nuclear weapon testing, the released radioactive materials are likely to be transported through various environmental pathways as well as by humans and animals, including bees. Due to their foraging behaviors, bees frequently pick up environmental contamination from multiple sources, including contamination that has been deposited on a flower or the pollen.

This research responds to the public concerns about radioactive contamination in the environment. The objective is to develop a model of the honeybee hive using Monte Carlo N Particle (MCNP) computer code, and calculate absorbed fractions for multiple energies and multiple incident radiation types. Given the critical role that the honeybee plays in the ecosystem, this model would be valuable to the radio-ecological community for dose calculations in the environment. Through their daily routines of collecting pollen, the honeybee may contact radioactive material and subsequently

contaminate its hive. The model described herein serves as a template for further development. Additionally, this research could be used to better understand the movement of nectar and pollen throughout the hive, consider partitioning of radionuclides in insects, and speculate how much radiation deposited on a flower or pollen is ultimately collected by bees.

©Copyright by Junwei Jia  
March 13, 2017  
All Rights Reserved

Beehive Model Creation for Use in Determining Radiation Dose to Beeswax and Bee  
Larvae

by  
Junwei Jia

A THESIS

submitted to

Oregon State University

in partial fulfillment of  
the requirements for the  
degree of

Master of Science

Presented March 13, 2017  
Commencement June 2017

Master of Science thesis of Junwei Jia presented on March 13, 2017

APPROVED:

---

Major Professor, representing Radiation Health Physics

---

Head of the School of Nuclear Science and Engineering

---

Dean of the Graduate School

I understand that my thesis will become part of the permanent collection of Oregon State University libraries. My signature below authorizes release of my thesis to any reader upon request.

---

Junwei Jia, Author

## ACKNOWLEDGEMENTS

Foremost, I would first like to thank my thesis advisor Dr. Kathryn Higley, School Head of School of Nuclear Science and Engineering at Oregon State University, who always help whenever I ran into a problem or had a question about my research. Her expertise, understanding, support and generous guidance made it possible for me to work on the research that was of great interest to me.

I would also like to thank Dr. Miguel Goni and Dr. Ramesh Sagilli from Oregon State University for their expertise and technical support in the implementation, and providing the beeswax samples. Without their passionate participation and input, this research could not have been accomplished.

I am hugely indebted to Mr. Mario Enrique Gomez Fernandez for being so generous as to provide a helping hand on MCNP code.

Finally, I wish to express my very profound gratitude to my wife and my parents for giving unfailing support and continuous encouragement to me during a difficult time.

This accomplishment could not have been done without them.

# TABLE OF CONTENTS

	<u>Page</u>
1	Introduction..... 1
2	Literature Review ..... 5
2-1	Humans and Nonhuman Biota..... 5
2-2	International Commission on Radiological Protection..... 5
2-2-1	Concept of ICRP Environmental Protection on Animals and Plants .... 6
2-2-2	Methodology of ICRP Environmental Protection..... 6
2-2-3	Homogeneous Model Pick ..... 10
2-3	Dose Concept..... 12
2-3-1	Absorbed Fraction and Specific Absorbed Fractions..... 12
2-3-2	Modelling Assumptions ..... 13
2-3-3	The Calculation of Dose Conversion Factors (DCFs) ..... 14
2-4	Voxel Phantoms Concept ..... 15
3	Methodology of Apparatus and Application ..... 17
3-1	Micro Computed Tomography (CT) Imaging of Honeycomb ..... 17
3-2	3D-DOCTOR..... 18
3-3	Voxelizer ..... 19

## TABLE OF CONTENTS (Continued)

	<u>Page</u>
3-4 MCNP Simulation of Voxel-Based Phantom.....	20
3-4-1 Cell Card .....	22
3-4-2 Surface Card.....	22
3-4-3 Material Card.....	22
3-4-4 Data Card.....	23
3-5 Ultra-micro Balance .....	24
3-6 Elemental Combustion System 4010.....	25
3-7 Data Analysis.....	26
4 Results and Discussion .....	29
4-1 CHNS-O Analysis .....	29
4-2 Absorbed Fractions.....	34
4-2-1 Electron Source in Larvae and Beeswax.....	34
4-2-2 Photon Source in Larvae and Beeswax.....	36
5 Summary and Conclusions .....	39
Reference .....	41

## TABLE OF CONTENTS (Continued)

Appendices.....	44
A. Absorbed Fractions of Electron Energy Using Larvae Tissue Composition ..	44
B. Absorbed Fractions of Photon Energy Using Larvae Tissue Composition ....	46
C. Absorbed Fractions of Electron Energy Using ICRU Four-Component Human Soft Tissue .....	48
D. Absorbed Fractions of Photon Energy Using ICRU Four-Component Human Soft Tissue .....	50
E. Differentiation of Absorbed Fraction of Photon Energy .....	52
F. Differentiation of Absorbed Fraction of Electron Energy .....	54
G. Organic Elemental Analysis for Bee Larvae .....	56
H. MCNP Input Code with Source in Bee Larvae: Photon .....	58

## LIST OF FIGURES

<u>Figure</u>		<u>Page</u>
1	Figure 2-1 Framework of radiation protection for the public.....	8
2	Figure 2-2 Framework of nonhuman biota radiation protection .....	9
3	Figure 2-3: Voxel object within a sphere .....	16
4	Figure 3-1: Contouring phantom model of honeycomb and larvae.....	18
5	Figure 3-2: Three-dimensional model of the honeycomb in 3D-DOCTOR...	19
6	Figure 3-3: Sartorius SE2 Ultra-micro balance .....	25
7	Figure 3-4: Costech ECS 4010 CHNS-O Elemental Analyzer .....	26
8	Figure 3-5: Standard error of 12 samples .....	27
9	Figure 3-6: Standard error of 24 samples .....	28
10	Figure 4-1: Differentiation of Absorbed Fraction of Electron Energy, Source in Larvae .....	30
11	Figure 4-2: Differentiation of Absorbed Fraction of Electron Energy, Source in Beeswax .....	31
12	Figure 4-3: Differentiation of Absorbed Fraction of Photon Energy, Source in Larvae .....	33
13	Figure 4-4: Differentiation of Absorbed Fraction of Photon Energy, Source in Beeswax .....	34
14	Figure 4-5: Absorbed Fraction of Electron Energy, Source in Larvae.....	35
15	Figure 4-6: Absorbed Fraction of Electron Energy, Source in Beeswax .....	36
16	Figure 4-7: Absorbed Fraction of Photon Energy, Source in Larvae .....	37
17	Figure 4-8: Absorbed Fraction of Photon Energy, Source in Beeswax.....	38

## LIST OF TABLES

<u>Table</u>		<u>Page</u>
1	Table 1-1: Selected Reference Animals and Plants .....	11
2	Table 1-2: Average Organic Elemental Weight in Larvae Tissues .....	29
3	Table 1-3: ICRU Four-component Human Tissue Composition.....	30
4	Table 1-4: Fraction of the Total Number of Electrons Associated with Each Element .....	32

## 1. Introduction

Release of anthropogenic radionuclides into the environment is of primary interest for radioecologists and environmentalists. This release occurs through various avenues; the most prominent are radiological accidents (radioactive spills, reactor accidents, human error) and nuclear weapons testing (United States Nuclear Tests, 2000). These unstable anthropogenic radionuclides move through the environment according to physical and chemical pathways of transport where they can settle on surfaces and subsequently undergo radioactive decay. This decay energy can be potentially deposited in living tissue, thus increasing the risk of adverse health effects associated with exposure to ionizing radiation. Cancer, is generally considered to be the most worrisome health effect of exposure to radiation in humans (Davenport, 2008). But for non-human biota, direct effect, such as reproductive effects, has been of greater interest.

*Apes Mellifera* or the common honeybee plays a critical role in the environment as a common pollinator. This proves to be an invaluable ecological role. The average worker bee typically constitutes 90-98 percent of the total population of the hive. Worker bees produce four main products during their lifetime: beeswax, beebread, honey and royal jelly (Winston, 1987). These products are crucial to the well-being of the hive, if they become contaminated by radionuclides, the hive lifecycle and its food chain could be affected.

Beeswax is a crucial product produced by *Apis Mellifera*. Beeswax is used for most of the structural and storage needs of the hive, and is mixed with resin from surrounding plants to form propolis, a sealant of sorts for the hive. Beeswax is produced

from wax glands located on the ventral thorax of each honeybee. It is primarily made up of hydrocarbons, monoesters, diesters, and fatty acids. Beeswax is also a place to store honey (Winston, 1987). The wax could be contaminated by radionuclides that bees have brought into the hive with collected pollen. There is little research on the process of how a bee assimilates radionuclides and the potential for their distribution in hive products such as beeswax. Due to a wide variety of uses for beeswax from cosmetics, candles, food additives, pharmaceuticals to ornamental decorations, beeswax is an important product to consider when viewing the contamination of the hive itself.

Bee bread is produced from the pollen of the plants that a bee lands on. The pollen is then mixed with saliva and nectar. This product is stored in the hive and fed to the bees and their brood throughout the bee lifecycle. Since it is collected from flowers, the possibility that it could become contaminated by radionuclides released into the air is very high. Any radionuclides that settle on flowers can not only irradiate the bees themselves, but also the hive inhabitants whom ingest the contaminated bee bread. Bee bread is also a popular homeopathic supplement, and is considered the world's first health supplement since its introduction by early Egyptians and Chinese (Winston, 1987). This leads to more far reaching routes of exposure beyond the bee or hive itself.

Honey is the third and most widely known product of the honeybee hive. This product is produced in the greatest volume and is commonly used worldwide. Honey is a dehydrated form of the nectar of flowers. The nectar is collected by the bees and distributed in the cells of the honey comb. The nectar is then consumed and regurgitated

by the collective hive, until the nectar is partially digested. In this form, it is left in the cells of the hive, which is kept at a relatively high temperature and low humidity. The nectar is naturally dehydrated by the microclimate of the hive. At its final stage of production, the bees will cap off the individual cell that is full of honey to allow the bees to store the honey as food reserves for the colder months of the year (Winston, 1987). This stored reserve is what is collected by beekeepers around the world and is used in countless applications including food preparation and storage, cosmetics, and pharmaceuticals. Because bees play an important role in the production and processing of honey, either through acts of consuming or regurgitating the nectar or through maintaining and capping off the cells, the honey or nectar could become contaminated with radionuclides introduced by affected bees.

Royal jelly is another product of the *Apis Mellifera* hive. Royal jelly is primarily a food source for the young brood of the hive. However, in the case of a queen bee, it is the substance that promotes the development of the fertile sexual organs that distinguishes a queen from the non-fertile worker bees. Royal jelly is produced from specialized secretion glands in the heads of all bees and is composed of water, crude protein, amino acids, simple sugars and fatty acids. Royal jelly is also a commonly consumed item amongst certain groups of human beings, either as a cosmetic additive or as a dietary supplement (Winston, 1987). Little is known about the possibility of radioactive contamination due to limited information regarding the production of royal jelly by bees.

The honeybee is also the only reference insect of the reference plants and organisms chosen by the International Commission of Radiological Protection

Publication 108 (ICRP, 2008). Honeybees can be found in the wild or commercial bee operations used to produce honey and pollinate crops around the world. The juveniles stay in the honeycomb until developed, getting nutrition from the honey surrounding it (Snodgrass, 1956). Through the natural process of gathering nectar and pollen, the honeybee contacts with various surfaces, thus allowing for the potential transport of radionuclides into the hive. This provides a means for radionuclides to become fully integrated into the matrix of the comb. The various components that reside in the hive such as beeswax, honey, nectar and royal jelly are commonly used in everyday life, and are at risk of radionuclide contamination due to interaction with bees. These issues compound to create a serious problem for the honeybee population as well as other living organisms that make use of products created by honeybee.

To consider radionuclide contamination and calculate dose to juvenile bees, it is necessary to model the juvenile bees within the comb receiving dose from the honey that surrounds them. The goal of this thesis work is to build a working voxel model of honey beehive with MCNP code, and understand radiation interaction in nonhuman biota.

## **2. Literature Review**

### **2-1 Humans and Nonhuman Biota**

Radioprotection has historically assumed that human protection can be equated with protection of nonhuman biota. There are commonalities in the effect of ionizing radiation for human and nonhuman biota due to the similarities of damage caused at the molecular level, such as ionization of DNA, RNA and proteins, which can break chemical bonds, produce free radicals and can modify the regular cellular processes. However, differences in radio-sensitivity (e.g., bioaccumulation and behavior), specific exposure pathways (e.g., root uptake or foraging behaviour), and secondary effects (e.g., food supply reduced) can cause unique biological effects for nonhuman biota (Bréchnignac 2001).

### **2-2 International Commission on Radiological Protection**

The International Commission on Radiological Protection (ICRP) is the international body that provides guidance in protection against ionizing radiation. In 1928, ICRP was established at the Second International Congress of Radiology. ICRP consists of the Main Commission, Scientific Secretariat, and five standing committees. The Committee 5 was established to ensure that “development and application of approaches to environmental protection are compatible with those for radiological protection of man, and with those for protection of the environment from other potential hazards” (ICRP 2010). The obligation of Committee 5 is to estimate radiation exposure of Reference Animals and Plants, and to use the framework from human protection to develop a non-human biota framework for evaluating impacts from exposure.

### **2-2-1 Concept of ICRP Environmental Protection on Animals and Plants**

In 1975, the radiation protection community employed the concept of a reference human is to create points of benchmarks for dose estimations and consider the relation between doses to the human body and their effects. In 2007, the Commission decided to use a similar system by defining “Reference Animals and Plants”, so as to assess radiation effects in non-human biota. This methodology established a representative organism as a systematic means to create points of reference relating exposure to dose, and dose to effects that could apply to many different types of biota in different environmental situations. Early mortality, morbidity, reduced reproductive success, and observable chromosome damage were some of the relevant effects used to tie dose to effect. The purpose of the Reference Animals and Plants therefore was to create a framework that can examine and understand the relationships between exposure and dose under different exposure situation. This framework in Reference Animals and Plants are analogous the framework used for Reference Man for establishing and evaluating different exposure situations (ICRP, 2008).

### **2-2-2 Methodology of ICRP Environmental Protection**

To give high-level guidance and advice, the Commission provided a common approach to improve the overall framework for radiation protection. Thus, the Commission included three exposure situations in the 2007 Recommendations (ICRP103, 2007): planned, existing and emergency exposure circumstances. Planned

exposure situations are anticipated circumstances and therefore expected to have controlled exposure conditions. This would require a certain level of exposure to radiation to occur due to operation of a source. Existing exposure situations are where the exposure conditions are already present and a decision on control needs to be taken. Emergency exposures refer to unexpected situations that require immediately action. This framework was developed to make the decision on the level of control of exposure, identify the actions that would reduce exposure, and to assist both emergency and existing exposure situations.

The methods used to assess dose to people were based on the concept of ‘Reference Man’: a stylized and well documented set of human characteristics and data, centered on the protection of relating exposure to dose, and dose to effect. Within this concept, the voxel phantoms (see **2-4 Voxel Phantoms Concept**) were developed to compute mean absorbed dose to a reference male and reference female human (as well as infants and children). For that reason, the Commission provided advice in the form of dose limits, dose constraints and reference levels, as shown in Figure 2-1.

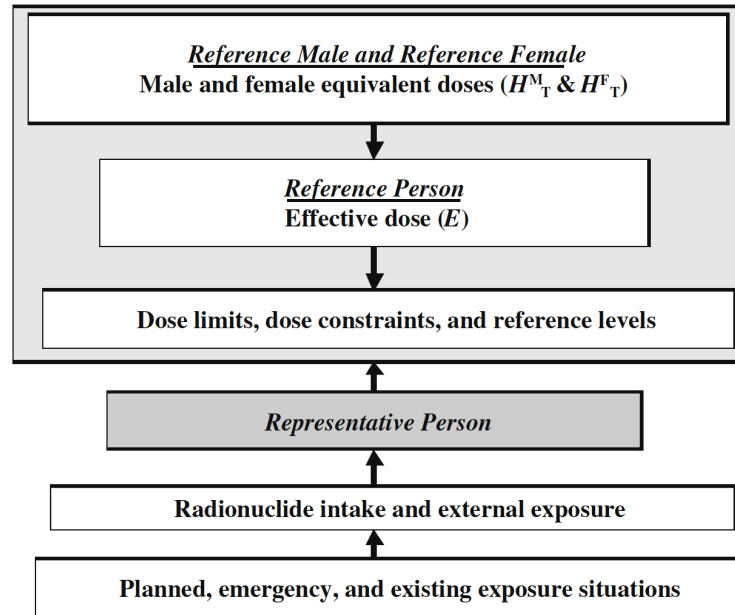


**Figure 2-1 Framework of radiation protection for the public (Pentreath 2009)**

In an environmental context, the effects of radiation on biota are difficult to assess simply due to exists many different species and varying ecosystems. But the ICRP adapted conceptual model to non-human biota. Figure 2-2 shows the conceptual relationship between various points of reference for evaluating protection of the environment.

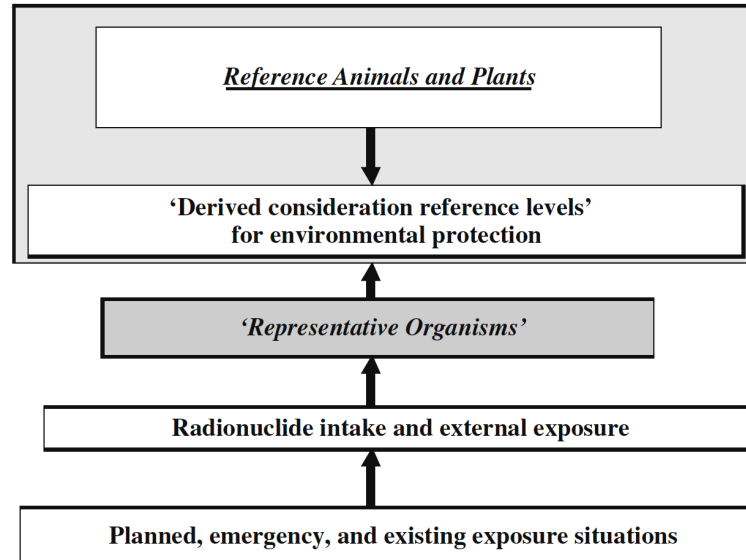


**Figure 2-2 Framework of nonhuman biota radiation protection (Pentreath 2009)**

Although the overall framework that was developed for the environment is parallel with the framework of the protection of human, the similarities are limited due to lack of relevant data and nature of the dynamics of animals and plants populations. Comparing Figure 2-1 and Figure 2-2, the former uses the Reference person to develop dose limits, constraints, or reference level, with which exposure of a representative person might be compared for assessment. The framework for non-human biota does not contain limits and instead contains “Derived Consideration Reference Levels”. According to ICRP Publication 108, Derived Consideration Reference Levels (DCRLs) can be considered as “a band of dose rate within which there is likely to be some chance of deleterious effects of ionizing radiation occurring to individuals of that type of Reference Animal or Plant, derived from a knowledge of defined expected biological effects from that type of organism that, when considered together with other relevant information, can be used as a point of reference to optimize the level of effort expected

on environmental protection, dependent upon the overall management objective and the exposure situation” (ICRP 2008).

In general, DCRLs for each Reference Animal and Plant are based upon biological effects which reflect the radio-sensitivity of the different Reference Animal and Plant species. Thereby, DCRLs should not be considered as a final stage of process, but more as a guide in a more considered level of assessment of the situation.

### **2-2-3 Homogeneous Model pick**

There is no simple method to provide the comprehensive biological background to all species potentially impacted by radioactive releases. Instead, the Reference Animals and Plants were chosen to represent as broad a range of ecosystems as possible. The following selected organisms identified by the ICRP were considered merely representative of the terrestrial and aquatic environments. Regarding selected organisms, each of Reference Animals and Plants follows the criteria below (ICRP, 2008):

- Reasonable amount of radiobiological information
- Amenable to future research
- Representative fauna or flora and wide geographic variation
- Most likely expose to radiation
- Use relatively simple geometries to model
- Public or political resonance

Finally, the following species were chosen in ICRP 108:

<b>Animal</b>	<b>Environment</b>
Deer	Terrestrial/Large Mammals
Rat	Terrestrial/Small Mammals
Duck	Terrestrial/Aquatic/Birds
Frog	Terrestrial/Aquatic/Amphibian
Trout	Aquatic/Freshwater Fish
Flatfish	Aquatic/Marine Fish
Bee	Terrestrial/Insect
Crab	Aquatic/Large Marine Crustaceans
Earthworm	Terrestrial/Annelids
<b>Plants</b>	<b>Environment</b>
Pine Tree	Terrestrial/Conifers
Wild Grass	Terrestrial/Grasses
Brown Seaweed	Aquatic/Algae

Since honeybee is only reference chosen by ICRP, the beehive study is significant for multiple reasons, especially considering the Fukushima accident in Japan. Each cell of a honeycomb is built by bees from specialized wax secretion glands located on the dorsal thorax of each bee (Snodgrass, 1956). As such, the day to day operations of the hive can contain the entry and egress of thousands of bees, which can potentially become contaminated by radionuclides in the environment. Whether in the wild or part of a commercial operation, bees live in communities called colonies, which lay their eggs within the honeycomb of the hive. Honeybees collect nectar to make honey to sustain development of their young and the colony over the winter months (Winston, 1987). In this case, bees could concentrate radionuclide contaminants from the plants, and transfer to juvenile bees. Thereby, it is important and necessary to model the juvenile bees within the comb.

## 2-3 Dose Concept

Basically, the key calculation of exposure to ionizing radiation is the absorbed dose, which is the amount of energy from ionizing radiation deposited in a unit mass of tissue of an organ or organism. Different types of radiation, such as alpha, beta, gamma radiation, neutrons, heavy ions or fission fragments, through energy deposition imparts dose to living tissue. For the same absorbed dose, different types of radiation can produce different degrees of effect in the same biological tissue (ICRP, 2008). Also, absorbed fraction is a critical quantity for estimating internal dose.

### 2-3-1 Absorbed Fraction and Specific Absorbed Fractions

Absorbed fractions (AFs) and specific absorbed fractions (SAFs) are important values in the calculation of radiation dose from the intake(s) of radionuclides and consequently important to internal dose estimate, which both account for the partial radiation energy deposition in target organs.

Absorbed fraction is energy imparted to a target volume T from source region S divided by the energy emitted from source region, but only for target regions that are volumes. The following Equation 1 shows AFs calculation:

$$\phi(T \leftarrow S) = \frac{(\rho V)_t D(T \leftarrow S)}{\langle E \rangle S_{total}}$$

*Equation 1: Absorbed fractions*

where  $(\rho V)_t$  is the target density and volume,  $D(T \leftarrow S)$  is the average absorbed dose rate,  $\langle E \rangle$  is the average radiation emitted per source particle, and  $S_{total}$  is the total number of particles emitted by source region (Shultis & Faw 2000).

Specific absorbed fractions for any target region have the superiority in the point target (Loevinger & Berman 1976). The SAF is the absorbed fraction divided by the mass of target:

$$\Phi(T \leftarrow S) = \frac{\phi(T \leftarrow S)}{m_t}$$

*Equation 2: Specific absorbed fractions*

Under certain circumstances, each has its advantages. For instance, when most energy absorbed in single target, the SAFs are relatively insensitive to size and shape of source and target that is not the case for small organisms.

### **2-3-2 Modelling Assumptions**

Given the complexity of the process in estimating doses to organisms and tremendous variability of organisms, it is impossible to consider all radiation exposure conditions. Thus, the models should be based on typical assumptions as follows:

- AFs are only calculated for beta and gamma emitters, because of the short range of alpha, the exposure is usually not considered for alpha particles.
- In all models, the simulation of mono-energetic electrons or photons with energies range are from 0.01 to 5 MeV. The data of other energy values in the range are interpolated.
- Uniformly contaminated volume sources are assumed for the calculations of AFs for target.
- All densities are assumed to be 1g/cm<sup>3</sup>.
- Larvae tissue composition is assumed to be ICRU four component human soft tissue.

- For internal exposure, the radioactivity is assumed to be homogeneously distributed in the whole body, and not in specific organs (Ulanovsky & Pröhl 2008).
- For external exposures calculation, a variety of source-target relationships are considered (Ulanovsky & Pröhl 2008).

### 2-3-3 The Calculation of Dose Conversion Factors (DCFs)

In a simplified method, the organism is assumed to be located in an infinite homogeneous medium with the source uniformly distribution in its body, and the densities of the medium and the organism are the same. Under these situations, DCFs are defined based on absorbed dose rate per activity concentration within the organism or externally in the medium (Loevinger & Berman 1976). Both  $DCF_{\text{int}}$  and  $DCF_{\text{ext}}$  can be calculated by using Equation 3 and Equation 4:

$$DCF_{\text{int}} = \sum_{\nu} \left( \sum_i E_i Y_i \phi_{\nu}(E_i) + \int N_{\nu}(E) E \phi_{\nu}(E) dE \right)$$

*Equation 3: Internal DCF*

$$DCF_{\text{int}} = \sum_{\nu} \left( \sum_i E_i Y_i (1 - \phi_{\nu}(E_i)) + \int N_{\nu}(E) E (1 - \phi_{\nu}(E)) dE \right)$$

*Equation 4: External DCF*

where  $\nu$  indicates radiation type;  $E_i$  is energy in MeV;  $Y_i$  is yield of the discrete energy radiations per decay of the radionuclide;  $N_{\nu}(E)$  is the energy spectrum for continuous energy radiations, used for beta particles only; and  $\phi_{\nu}(E)$  is the absorbed fraction

(Loevinger & Berman 1976; Shultis & Faw 2000). However, in this research, the DCF equation can be simplified and expressed as Equation 5:

$$DCF = C \times \sum_i \bar{E} \times AF(\bar{E}, S \rightarrow T) \times BR \times Y$$

*Equation 5: Dose Conversion Factor*

where  $i$  indicates radiation type;  $\bar{E}$  is the average energy emission;  $AF(\bar{E}, S \rightarrow T)$  is the absorbed fraction of energy  $\bar{E}$  for source to target; BR is the Branching ratio; Y is the yield of the discrete energy; C is the activity concentration. The absorption fraction and activity concentration (C) could be changed by model size, densities, elemental composition, energy and the location of organism. Thus, there are three key objectives of the research:

- Create a voxel phantom model of a beehive
- Perform an organic elemental analysis of beeswax and larvae
- Evaluate the sensitivity of DCFs based on the elemental composition of the organism by comparing with the standard four-component human tissue composition.

## **2-4 Voxel Phantoms Concept**

Computational models (phantoms) is one of most advanced methods for calculating organ doses in the area of radiological research. It was developed and applied to human system as a reference for ionizing radiation dosimetry studies. For example, the model can use various material with different composition and density, and use of complex geometries as sources and targets (Zaidi and Xu 2007). The phantom model could be used as a guide to address the internal dosimetry of the

Reference Animals and Plants. The creation of a tomographic model includes 4 major steps (Zaidi and Xu 2007):

- Acquire a set of medical images
- Classify and segment the organs or tissues
- Specify tissue type and composition to organs to tissues
- Implement the geometric data to Monte Carlo code to calculate radiation transport

In general, a voxel phantom is compiled or constructed with a series of image slices from medical imaging such as computed tomography or magnetic resonance imaging, to form a volume pixel unit as shown in Figure 2-3.

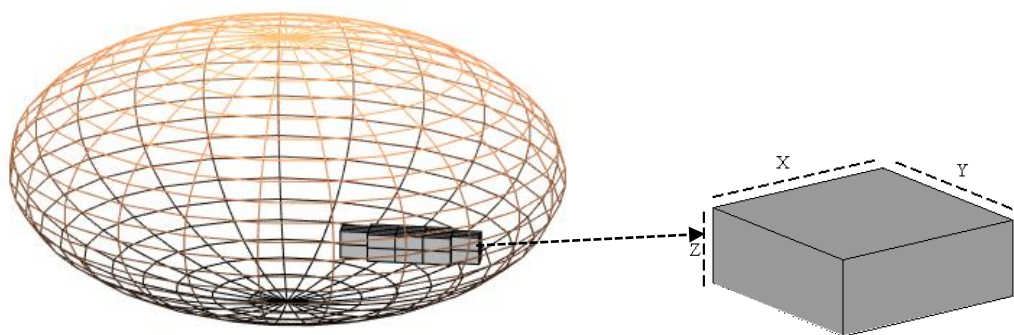


**Figure 2-3: Voxel object within a sphere (K. Higley et al. 2015)**

Figure 2-3 depicts an inner object representation of the internal structure of a voxel object. Also, this method allows future studies to conduct the interaction of particles through different components of an organism. With realistic shapes and composition, the phantom model provides an important improvement over homogenous model.

### **3. Methodology of Apparatus and Application**

#### **3-1 Micro Computed Tomography (CT) Imaging of Honeycomb**

Traditionally, computed tomography (CT) imaging techniques are used to create a virtual three-dimensional representation of the scanned object. CT imaging is a noninvasive procedure which provides anatomical details of bony structures and soft tissues. The cross-sectional images are two-dimensional scans of the imaged object; when combined, the compilation of a sequence of two-dimensional cross-sectional images forms a three-dimensional model of the object. CT imaging employs X-rays which will be absorbed by different tissue areas of the object as X-rays pass through the tissue (Hsieh, 2009). Volumes of tissues which absorb the delivered X-rays will reduce the number of X-rays that are incident on the detector.

Micro-CT is often used to image small animals and models. In comparison to traditional CT imaging, micro-CT is equipped with higher resolution, offering a more in-depth three-dimensional visualization. The fine-scale of imaging used in micro-CT allows analysis of physical and chemical properties of internal structures, including density and stress imparted on these structures (Hsieh, 2009).

The modeling of a beehive in this research employs micro-CT imaging of an actual commercial-grade honeycomb section. Micro-CT imaging of the honeycomb sample was completed at the Hewlett Packard (HP) facility in Corvallis, Oregon. Imaging of the honeycomb sample yielded over 2,000 slides within the CT scan. Of which, 400 slides were selected for further image analysis and construction of the honeycomb phantom. These selected slides were chosen based on the quality of the images and suitability for contouring and rendering in the program 3D-Doctor.

### 3-2 3D-DOCTOR

3D-Doctor (Able Software Corp) is an advanced 3D image rendering, processing and analysis software. It is a powerful image processing software that use a unique vector-based technique for faster 3D model creation and easy editing. 3D-Doctor was developed to provide efficient tools to process and analyze images, object boundaries and 3D models. One of these is a fully automatic image segmentation by using the regions of interest (ROI) to segment larvae tissue, it allows user to generate 3D rendering to visualize with loaded images (Able Software Corp, 2008). Figure 3-1 shows the ROI method in getting the contouring phantom model of honeycomb and bee's larvae.

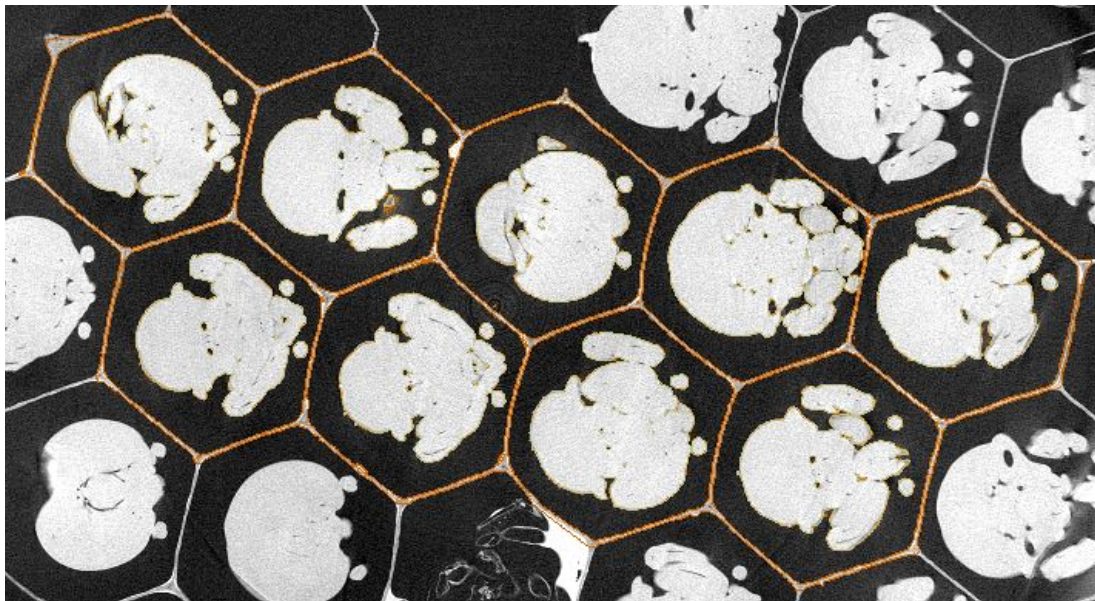


**Figure 3-1: Contouring phantom model of honeycomb and larvae**

Each of the 400 slides were modified and manipulated by hand to distinctly define the honeycomb cell wall and larvae units as their own separate layers for dose deposition calculation. Once contouring of all the components of all the slides were

completed, a voxel-based computational phantom of the hive sample was constructed. The constructed three-dimensional model of the honeycomb section generated in 3D-Doctor can be seen in Figure 3-2 below.

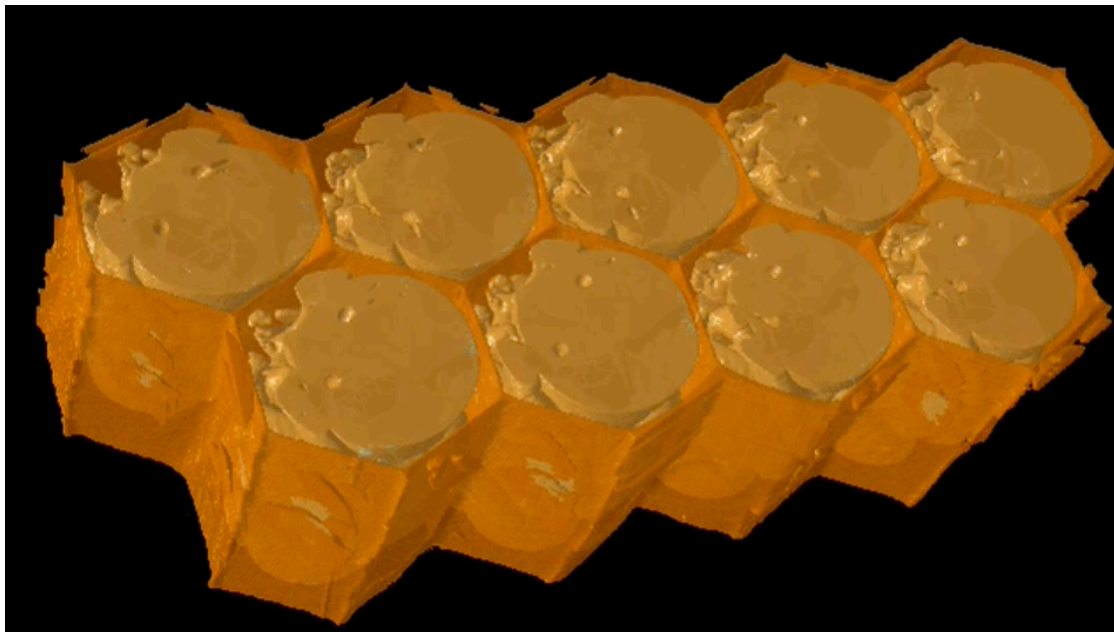


**Figure 3-2: Three-dimensional model of the honeycomb in 3D-DOCTOR**

In this research, 3D-Doctor is used to convert raw images stacks to virtual phantoms through the establishment of boundaries. These boundaries (“`.bnd`” file) can later serve as input for export and making a lattice in Monte Carlo code generator – Voxelizer (discussed in **3-3 Voxelizer**). In other words, one can convert a boundary file to a Monte Carlo input file that can be simulated by MCNP.

### **3-3 Voxelizer**

The final phase of this research requires MCNP simulation of the energy deposition of beta/gamma particles in a honeycomb filled with honey and bee larvae. To begin this phase, a geometric input into MCNP was created. Upon completion of

the rendering of the micro-CT scan of the beehive, a Voxel based computer software program – Voxelizer or Lattice Tool was utilized to convert contoured structure within image stacks, and form repeated structure format for use in MCNP simulations (Kramer et al. 2010).

The Voxel software was created by the HUMAN Monitoring Laboratory of Health Canada's National Internal Radiation Assessment Section (Kramer et al. 2010). This software is able to convert boundary lines and objects, which is achieved by reading the data from 3D-Doctor boundary file, into a repeated-structure for later Monte Carlo simulations. Voxelizer not only counts and reads the names of objects created in 3D-Doctor, it also can associate them to a universe in the lattice structure that forms the Monte Carlo input file. Voxelizer reads the (x,y) coordinates of node data of plane where the boundary is located, and places the matching nodes on a matrix grid, draws line between these nodes and closes boundaries after filling the room between each boundary with the material. The compression factor indicates how high detail the user wants to generate voxel models. Since the extremely large number of voxels is much beyond the capability of current PCs and/or MCNP, the available computer was only able to handle approximate 2% of maximum voxels. If the quantity of voxels was still more than MCNP could handle (maximum of 50 million voxels), then a reduction of resolution test is needed (Los Alamos National Laboratory, Volume II, 2003).

### **3-4 Monte Carlo N-Particle (MCNP) Simulation of Voxel-Based Phantom**

MCNP, a general-purpose Monte Carlo N-Particle code, provided for use

through the Los Alamos research lab, employs the use of textual inputs to assist in the calculations of several doses to a material. MCNP code was developed by Los Alamos National Laboratory, who owns rights to this code and distributes the code for use. It is internationally recognized for computer simulation of neutron, electron, and photon transport in a variety of mediums. This code is capable of calculating interactions of a radioactive particle, given different parameters around the radiation particle, such as cross section and flux information. This code has the ability to utilize both coherent and incoherent scattering for photons, including absorption in pair production with local emission of annihilation radiation. Electron/positron transport account for angular deflection from bremsstrahlung, Coulombic scattering, collisional energy loss, and secondary particles (Los Alamos National Laboratory, Volume I, 2003).

This code is universal and used for a variety of different nuclear applications due to the standard features, including criticality calculations and radiation transport simulations; the latter is the application that is required for this research.

The purpose of the Voxel software is to translate the three-dimensional model created in “3D-Doctor” into a computer code that can be easily understood by the MCNP program. Hours of monotonous adjusting of the compression factor associated with the computer code was required to create an MCNP input geometry file that was less than 5,000 Kbytes (Los Alamos National Laboratory, Volume II, 2003). This size requirement exists not for MCNP restrictions, but due to the limitations in computational hardware.

The input code for MCNP program requires four separate cards to function correctly; they are called the Cell Card, the Surface Card, the Material Card and the

Data Card. Contained in these four cards is all applicable information required for MCNP to simulate a beta/gamma particle bombardment into an object.

### **3-4-1 Cell Card**

The geometry of each cell is described on a cell card. In this case, the three cells are the larvae (Cell 1), the wall (Cell 2) and surrounding air (Cell 3). For each cell, various inputs are required in this card. These inputs are: cell number, material number, material density, and all applicable planes that are delineated in the next section. This allows for the combination of all surfaces to form a three-dimensional object. For example, Cell 1, in this input file, refers to this cell is to be filled with material 1 at a density of  $1\text{g/cm}^3$ . The photon and electron importance in Cell 1 are 1 (See sample in Appendices F).

### **3-4-2 Surface Card**

The surface card consists of the limiting planes associated with the cell card geometry. In other words, this section delineates the actual size of the Cell 1, Cell 2 and Cell 3 of the cell cards. The first entry on surface card is the assigned surface number, which begin in the first five columns of the card.

### **3-4-3 Material Card**

In the material card, the second entry is a cell material number that associates with the input cell card. When the cell is void, a zero is for the material number.

Otherwise, for the cell with a nonzero material number, the material density follows the material number.

The Material Card consists of the chemical composition of the materials involved in Cell 1, Cell 2 and Cell 3. Through elemental material analysis research, it was determined that the analogous chemical composition for Cell 1 (Larvae). For Cell 2 (beehive or beeswax), the analogous chemical composition is  $C_{46}O_2H_{92}$ . This data card input provides the atomic structure of the target surfaces so the cross-sections of the various atoms can be included in the simulation.

#### **3-4-4 Data Card**

The data card consists of a variety of inputs that are associated with the interaction of matter with radiation.

The first data card input is the “Mode” (MODE) that this code will run. For the research, the Mode will be in Photon/Electron (P E). This informs MCNP that it will be accounting for only Photon and Beta particles for this simulation.

The second data card input is the “Source Definition Card” (SDEF). The Source Definition Card provides various necessary radiation source parameters. The first parameter is starting energy (ERG), such as the energy is equal to 1 MeV. This is simply the chosen starting energy of the Beta and Gamma particle upon decay. The next parameter specifies the source particle type (PAR). For this research, the PAR used for photons (PAR = 2) and electrons (PAR =3). The following parameter is the efficiency, which is rejection efficiency criterion for positron sampling. Last X, Y, and Z is referred as coordinate positions.

The third data card input is the SI (source information) card and the SP (source probabilities) card for 3 cells, and the L option is used on the SI card that the entries associated with SP card are probabilities or cumulative probabilities on discrete values. SI4 is source location, which is defined as Source < Lattice Unit < Cell Containing the Lattice, such as 1<996<997 is the source placed in larvae.

The fourth data card input is the “Tally Type” (F). The Tally Type is, essentially, the information that is trying to be obtained in the simulation. For this simulation, the Tally Type is, F8: P, E. This mnemonic determines the output as “energy pulses created in a detector” for photons and electrons.

The final input into the data card is the “History Cutoff Card” (NPS). This card instructs MCNP to run a certain amount of iterations of the same energy and type as described in the previous inputs of the data card. For this simulation, 2,000,000 iterations were performed.

Following the creation of the MCNP input code, a command must be made through the computer’s operating system to run the MCNP program. For this simulation, the run script ran through the program, Terminal, on a MacBook pro. The command script was such as “mcp5 inp=LP001 outp=LP001o r=LP001r”, where LP001 was the input code file and LP001.o was the output file created by running the simulation.

### **3-5 Ultra-micro Balance**

This instrument is used to measure the weight of small samples with a capacity of 2.1g and +/- 0.1µg accuracy (Ultra-Micro Balance Sartorius SE2, n.d.). In this

research, the micro-balance weighted tiny larvae from the honeycomb, so that a COSTECH elemental combustion machine could be used to get elemental data.

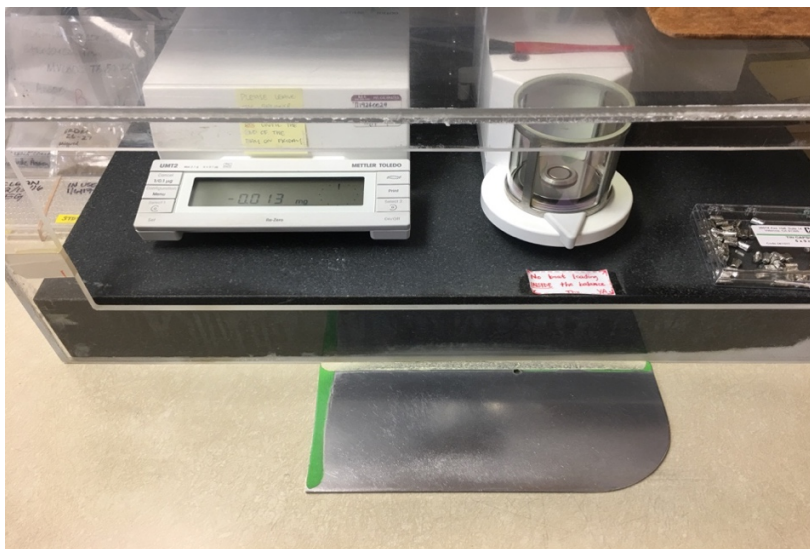


**Figure 3-3: Sartorius SE2 Ultra-micro balance**

### **3-6 Elemental Combustion System 4010**

This was designed for CHNS-O (Carbon, Hydrogen, Nitrogen, Sulphur and Oxygen) elemental analysis and Nitrogen/Protein determination, using an advanced “flash combustion/gas chromatographic separation and multi-detector techniques” (Elemental Combustion System, n.d.). The Elemental Combustion System 4010 consists of three modules: the combustion system, the detector system, and the data handling system.

The combustion system includes sampling, combustion and pneumatics. The second module is for measuring the combustion products. Gas chromatography separates these combustion gases for CHNS-O analysis, and N/protein determination or mass spectrometer for isotopic analysis. The third module is for instrument control, data acquisition and report generation, which is called Elemental Analysis System.

The main process of Elemental Analysis is to make sure that samples are small enough for the chromatographic method. Meanwhile, samples need to be placed in a tin boat and folded to protect from the surrounding environment.



Figure 3-4: Costech ECS 4010 CHNS-O Elemental Analyzer

### 3-7 Data Analysis

Before using the elemental composition data, it was necessary to ensure the data set had a good estimation with a low standard error. The standard error represents the spread that the true mean of a sample of a variable would have (McHugh, 2008). Thus, Equation 6 is applied that as sample size gets larger the standard error gets smaller.

$$SE_{\bar{x}} = \frac{\sigma}{\sqrt{n}}$$

*Equation 6: standard error of mean*

The elemental material analysis for bee larvae is from Dr. Miguel's material analysis lab. Based on my colleague Mario Gomez research work for elemental analysis lab

work (Gomez, 2016), the number of first trial was decided to use 12 samples to see whether the standard error reaches a plateau as Figure 3-5 shows:

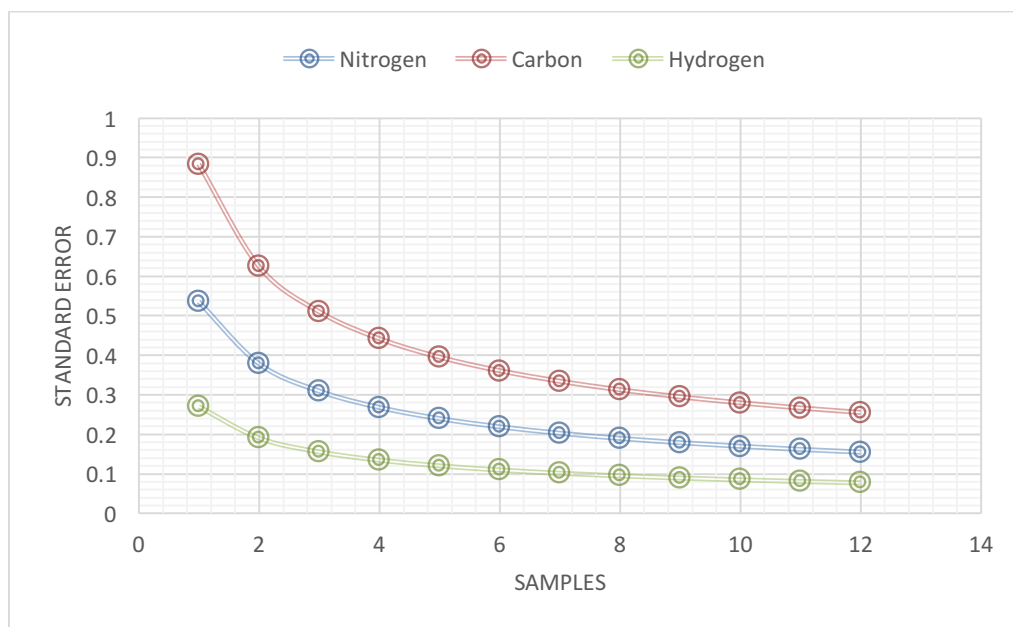


**Figure 3-5: Standard error of 12 samples**

The plot illustrated that more samples needed to reduce the standard error. Therefore, 12 more samples add to this plot, which Figure 3-6 shows:

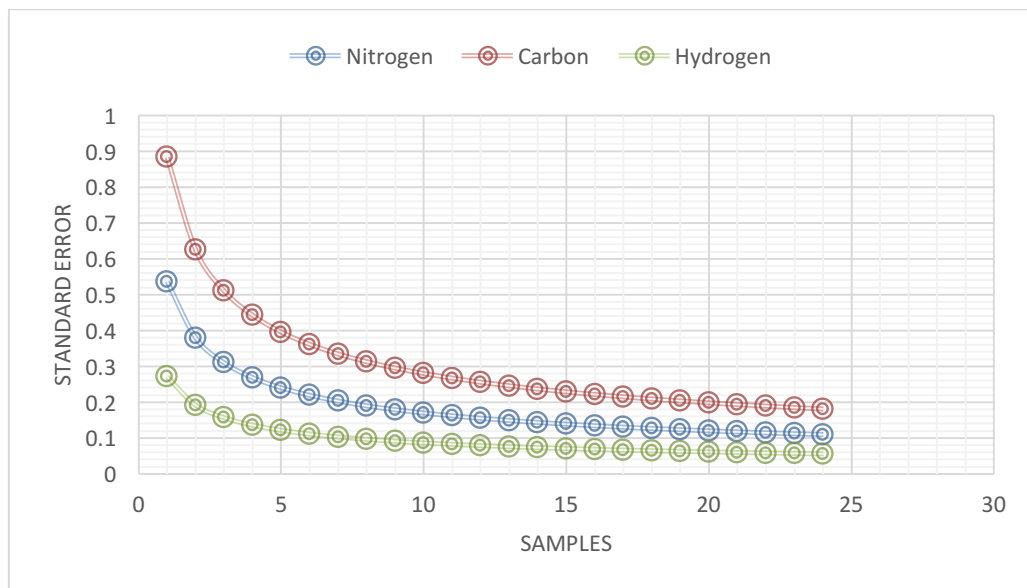


**Figure 3-6: Standard error of 24 samples**

Figure 3-6 indicates that the plot has reached a plateau and no more samples are needed to substantially reduce the standard error. 24 samples are good enough to prove elemental composition with a low standard error due to time and cost limitation.

The purpose of determination of organic tissue composition of larvae is to aid MCNP to generate more realistic results of radiation interaction. Moreover, it can be used to compare with human soft tissue composition (which is frequently used as the default tissue for many dose calculation) to see if the difference is important.

## 4. Results and Discussion

This research could be a useful information that allow the dose to be calculated for 75 radionuclides (ICRP, 2008), such as radionuclides:  $^{137}\text{Cs}$ ,  $^{90}\text{Sr}$ ,  $^{90}\text{Y}$ ,  $^{60}\text{Co}$ ,  $^{131}\text{I}$ ,  $^{226}\text{Ra}$ . Absorbed fractions for beeswax and larvae were computed at discrete energies of 0.1, 0.2, 0.4, 0.5, 0.7, 1.0, 1.5, 2.0 and 4.0 MeV for electron, and 0.01, 0.015, 0.02, 0.03, 0.05, 0.1, 0.2, 0.5, 1.0, 1.5, 2.0 and 4.0 MeV for photon respectively (assumed to be uniformly distributed throughout in the model). Meanwhile, the electron and photon were run on a multimode computer cluster at numbers sufficient to reduce uncertainties (coefficients of variation) in most absorbed fractions to 5% to 10% (Stabin et al., 2006).

### 4-1 CHNS-O Analysis

In order to complete MCNP input file of the general transport code, it is important to determine the organic tissue composition of bee larvae. In this study, there also have intended to discover the differentiation of tissues of bee larvae and human soft tissue that could impact analysis address dosimetry variable of the RAPs. The measurements of weight percentages contents of Carbon, Nitrogen, Hydrogen and Oxygen for bee larvae and ICRU four component human soft tissue, as shown in Table 1-2 and Table 1-3, respectively.

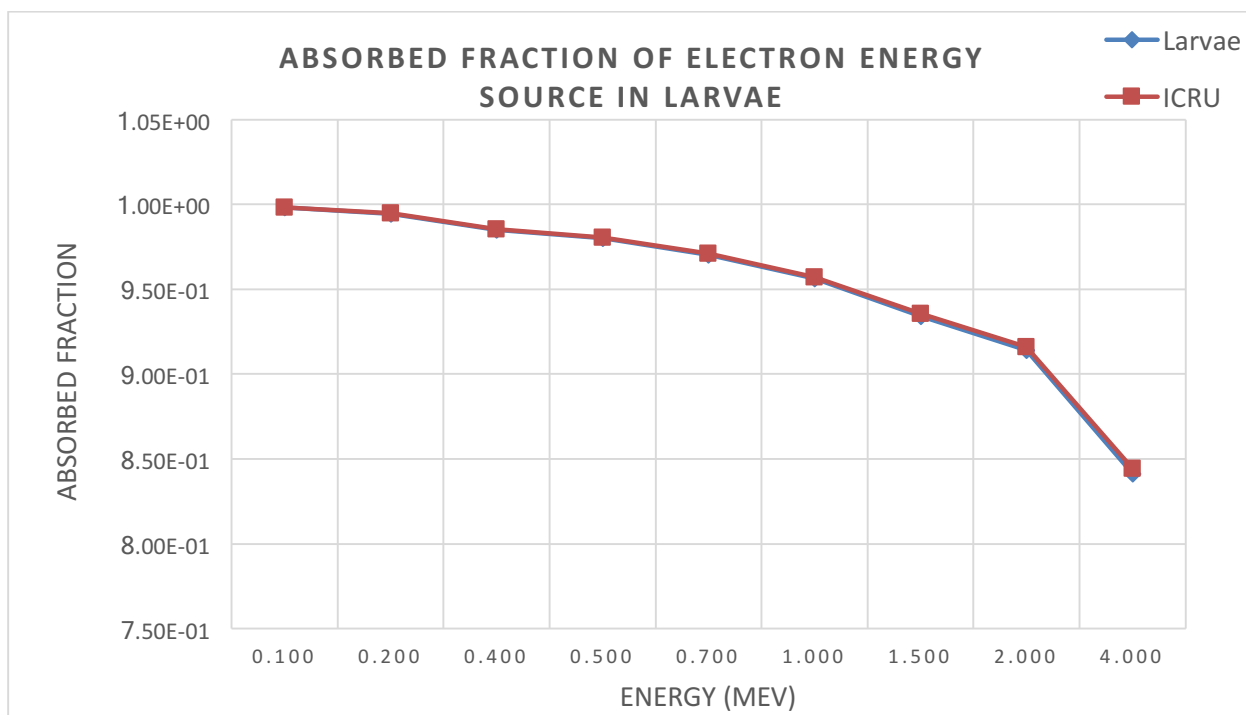
**Table 1-2 Average Organic Elemental Weight in Larvae Tissues**

	Weight (%)	Weight (%)	Weight (%)	Weight (%)
	Nitrogen	Carbon	Hydrogen	Oxygen
Honeybee larvae	4.85±0.15	48.37±0.25	7.40±0.08	39.38

**Table 1-3 ICRU Four-component Human Tissue Composition (Griffiths 1989)**

	Weight (%)	Weight (%)	Weight (%)	Weight (%)
	Nitrogen	Carbon	Hydrogen	Oxygen
ICRU soft tissue	2.60	11.10	10.12	76.18

The Figure 4-1 and Figure 4-2 show that the variation of absorbed fraction of electron energy curves between human soft tissue and measured larvae tissue compositions are very similar. When the source in larvae or ICRU, energy depositions are comparable due to electron has short path length. In addition, Figure 4-2 shows that more electrons can reach the larvae and deposit energy there with incident energy increases. Figure 4-1 illustrates that the small size of larvae diminishes deposited energy as incident energy increases.

**Figure 4-1: Differentiation of Absorbed Fraction of Electron Energy, Source in Larvae**

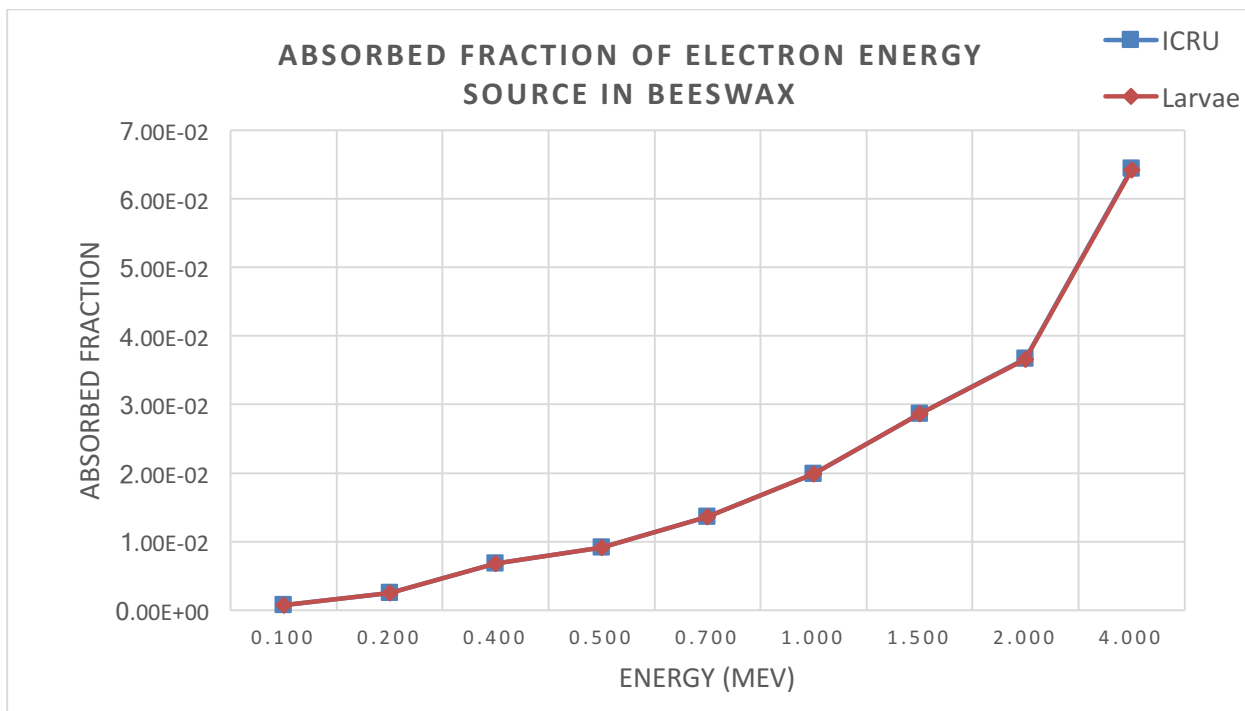


**Figure 4-2: Differentiation of Absorbed Fraction of Electron Energy, Source in Beeswax**

However, for photon with energies below 0.01 to 0.1 MeV, the absorbed fraction values appear to differ between the ICRU and realistic tissue composition. As Figure 4-3 shown, the voxel model with ICRU four component human soft tissue has slight higher AF than the realistic tissue when source is in larvae. Figure 4-4 demonstrated there have difference of absorbed fraction values between 0.015 and 0.5 when the source is in beeswax. Both sets of plots illustrate that human soft tissue composition has more energy deposited from low energy photon, which is attributed to photoelectric absorption mechanism, when the source is in human soft tissue. But there is a significantly increase value of absorbed fraction, which the range is from 0.01 to 0.05 MeV, for measured larvae composition tissue when source is in beeswax. In this case, the differentiation of energy deposited is caused by Zeff that a larger difference in effective atomic numbers was observed in photoelectric

and pair production regions (Singh and Badiger 2014). In this study,  $Z_{eff}$  is expressed as follows equation 7 (Murty 1965):

$$Z_{eff} = \sqrt[2.94]{\sum [f_n \times (Z_n)^{2.94}]}$$

*Equation 7: effective atomic number*

where  $f_n$  is the fraction of the total number of electrons associated with each element, and  $Z_n$  is the atomic number of each element.

$$f_{e,n} = \frac{\text{weight \%}}{\text{atomic weight}} \times \text{atomic number}$$

*Equation 8: electron fraction*

In this case, Equation 8 was used to calculate  $Z_{eff}$  for each of two types of tissue compositions as shown in Table 1-4.

**Table 1-4 Fraction of Total Number of Electrons Associated with Each Element**

	Weight (%)	Weight (%)	Weight (%)	Weight (%)
	Nitrogen	Carbon	Hydrogen	Oxygen
Honeybee larvae	4.85±0.15	48.37±0.25	7.40±0.08	39.38
$f_n$	0.045	0.450	0.138	0.367
Zeff- Larvae	6.69			
ICRU soft tissue	2.60	11.10	10.12	76.18
$f_n$	0.024	0.101	0.184	0.691
Zeff - Human	7.26			

The effective atomic number is important for predicting how photons interact with a substance, in this case, ICRU four components soft tissue  $Z_{eff}$  value is higher than Larvae's.

In other word, ICRU has higher cross section,  $\sigma_{PE}^{ICRU} > \sigma_{PE}^{Larvae}$ , this is the why the value of ICRU is always slightly higher than larvae before 0.5 MeV.

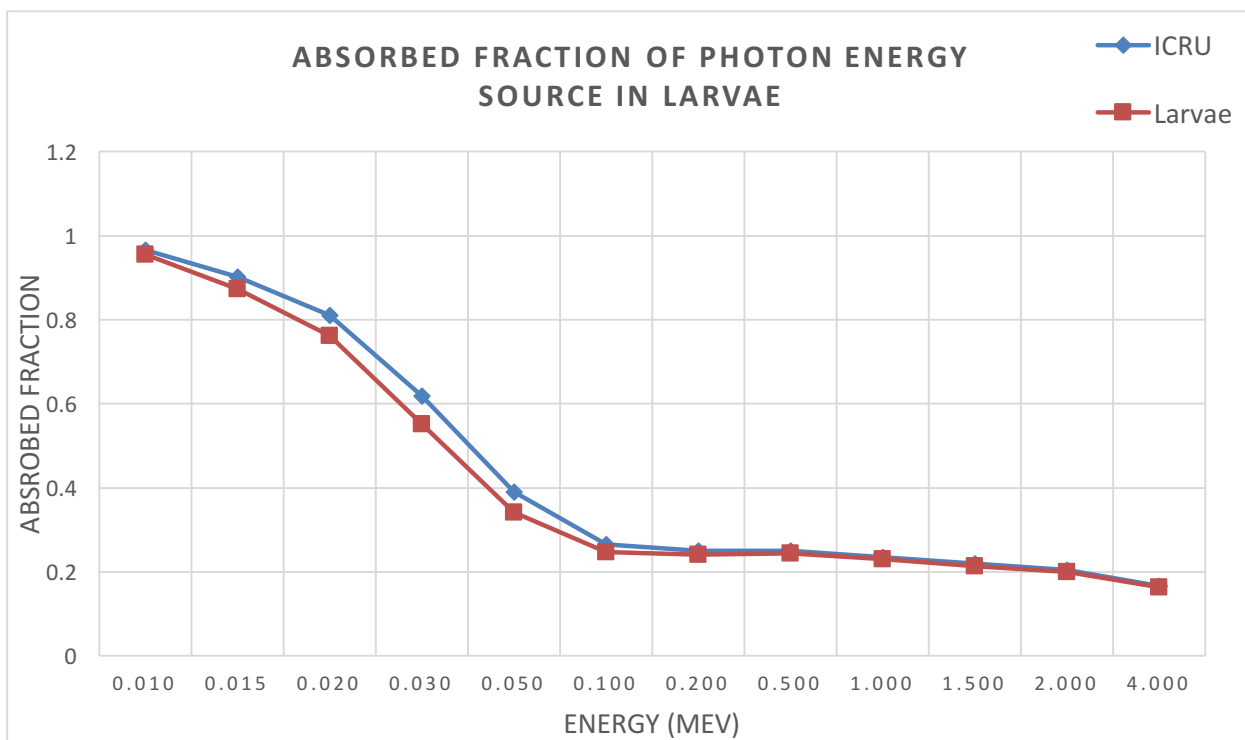


**Figure 4-3: Differentiation of Absorbed Fraction of Photon Energy, Source in Larvae**

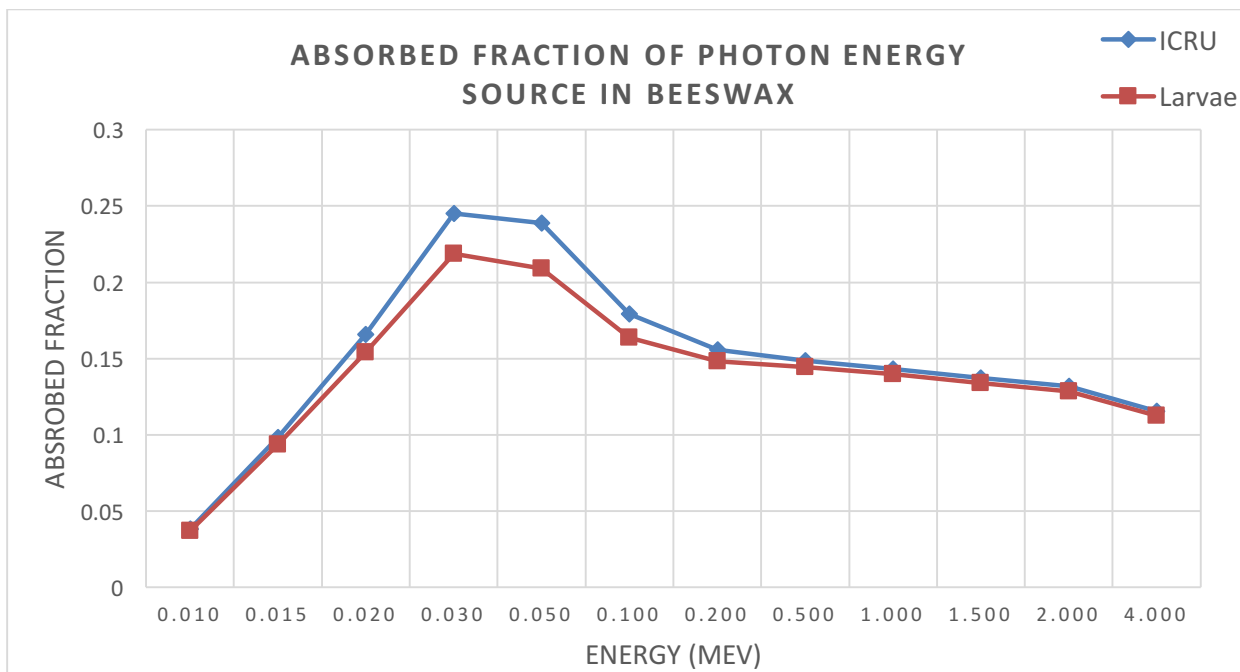


**Figure 4-4: Differentiation of Absorbed Fraction of Photon Energy, Source in Beeswax**

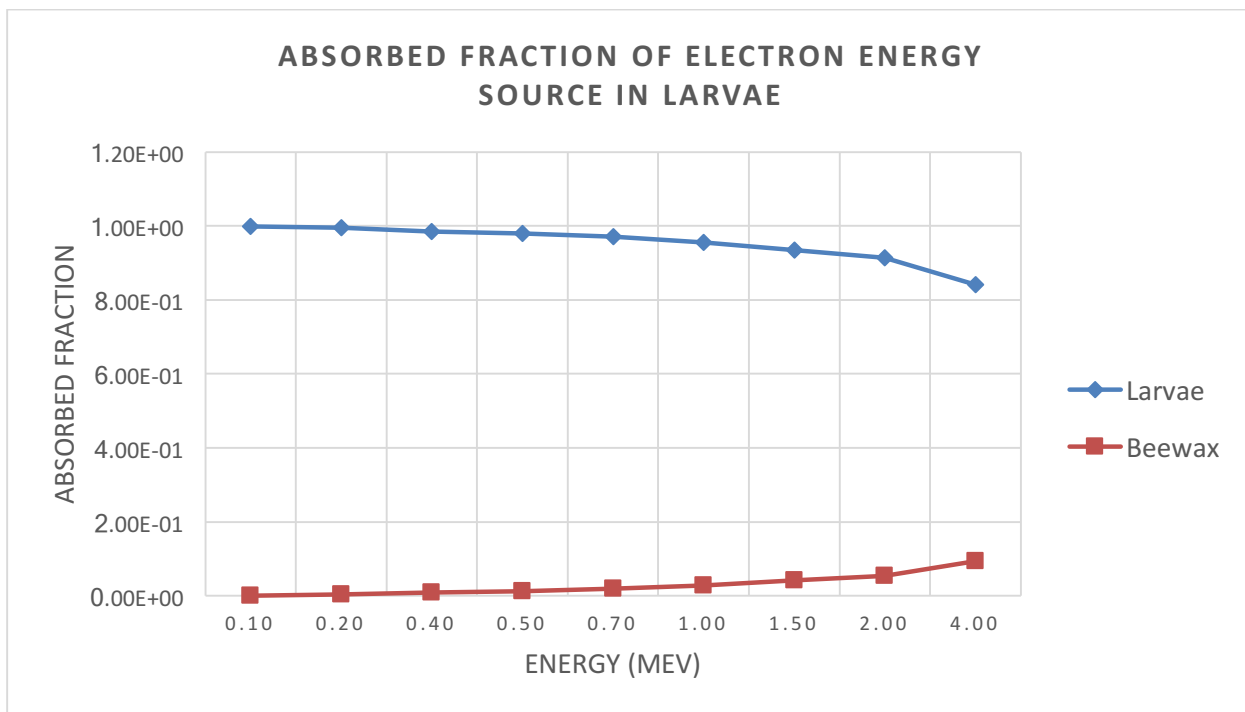
Figure 4-3 and Figure 4-4 also could illustrate that carbon has lower mass energy absorption coefficient than water due to weight (%) difference shown in Table 1-2 and Table 1-3.

## 4-2 Absorbed Fractions

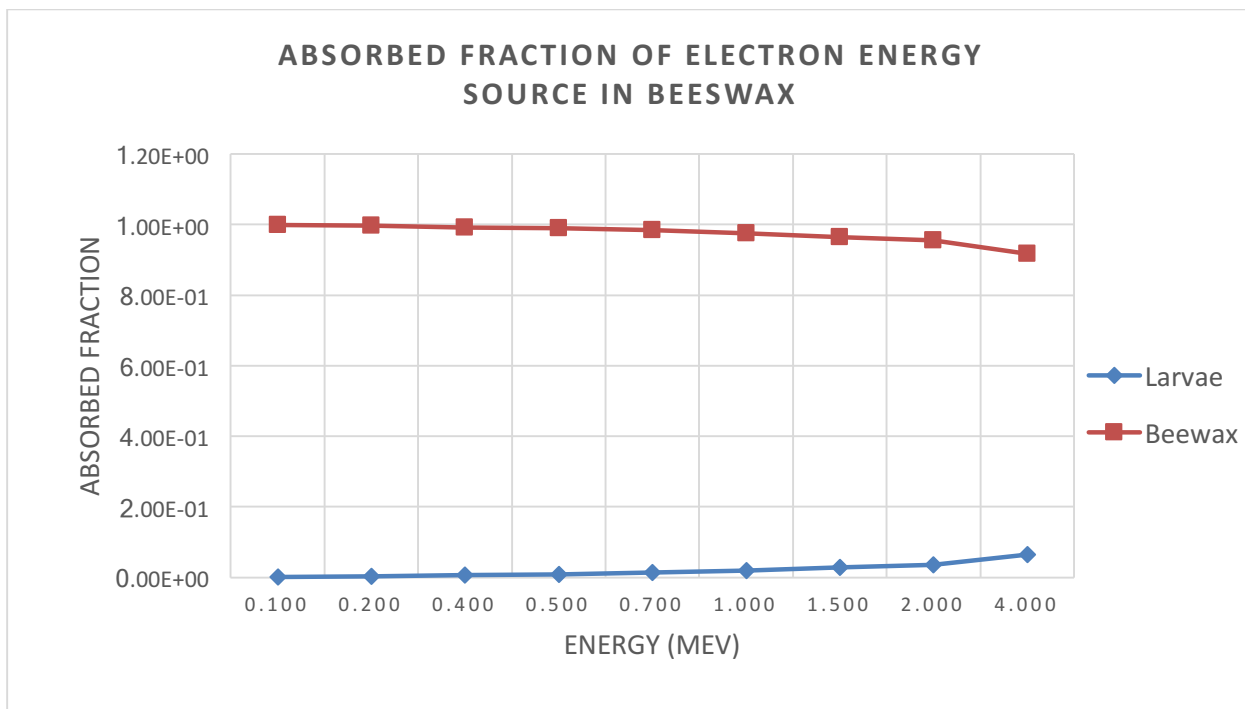
### 4-2-1 Electron Source in Larvae and Beeswax

Figure 4-5 and 4-6 show absorbed fractions of electron energy for the radiation source in the larvae and beeswax, respectively. As incident energy increases, the amount of energy deposited in the source organ decreases gradually, as illustrated in the decreasing absorbed fraction values as energy increases. On the contrary, the energy deposited in other organ gradually increases with increasing incident electron energy.

These two figures indicated that high energy electrons should be considered as having penetration capability for small organ dosimetry when energy over 0.2 MeV.



**Figure 4-5: Absorbed Fraction of Electron Energy, Source in Larvae**

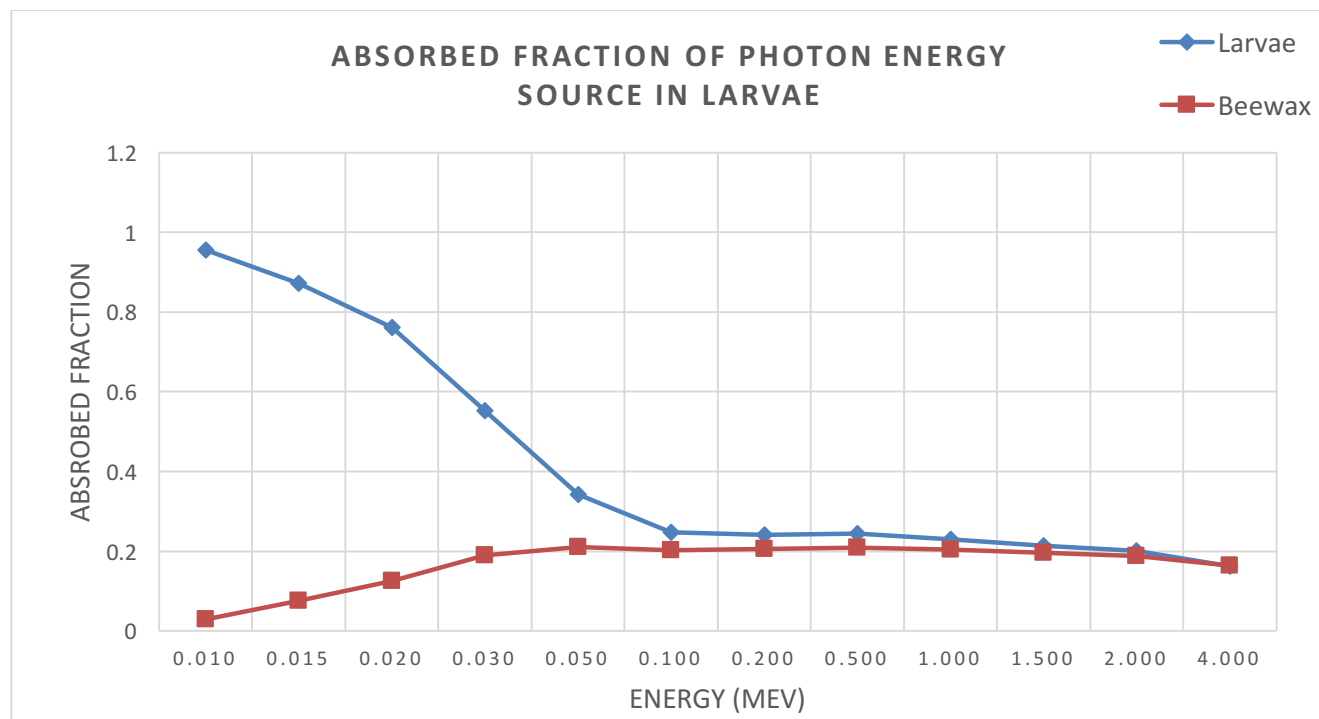


**Figure 4-6: Absorbed Fraction of Electron Energy, Source in Beeswax**

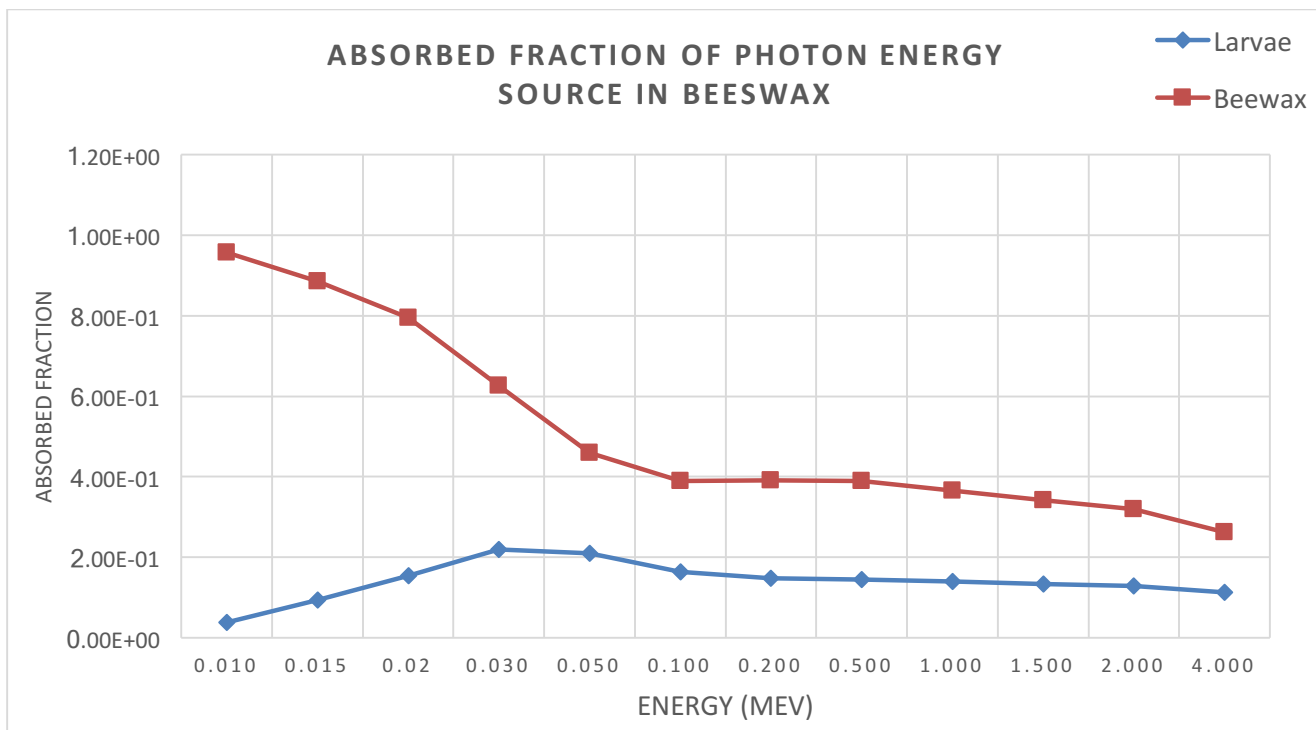
#### **4-2-2 Photon Source in Larvae and Beeswax**

Figure 4-7 and 4-8 show the absorbed fractions of Photon energy for radiation sources in larvae and beeswax, respectively. There are two different plots for the photon energy source in two different organs. For the source in larvae, as incident energy increase between 0.01 to 0.1 MeV, the amount of energy deposited in larvae organs decreases rapidly. For the source in beeswax, the two curves depicting a symmetrical appearance in that the source organ has a negative slope as incident energy increased and energy deposited in other organ increases gradually with increasing incident photon energy. But both plots appear to have a quasi-threshold value with increasing incident energy. This appearance is a term used in biology to explain the point at which a species or population change in density or number (Holmes et al., 2007). Not surprisingly,

photon show higher energy deposited at lower incident energies where the probability of photoelectric interactions. Photon will pass through the medium without any interactions as incident energy increases, therefore quasi-threshold shown.



**Figure 4-7: Absorbed Fraction of Photon Energy, Source in Larvae**



**Figure 4-8: Absorbed Fraction of Photon Energy, Source in Beeswax**

The voxel phantoms of this study could be used as a reference to apply internal dosimetry of the RAPs in a more practical way. However, the behavior of this organisms is substantially different with respect to humans, it is possible that the doses will be estimated incorrectly with the same assumption applying for humans. Since the research only compares the AF parameter, external exposure scenarios remain to be evaluated. Lastly, this research still needs experimental data so as to provide more accuracy estimation.

## 5. Summary and Conclusions

This research presents a more realistic and accurate approach to dosimetry of one of the ICRP RAPS – the bee (specifically the hive and larvae). The homogenous model used by ICRP can provide some insight into potential exposure, but the voxel model provides greater opportunity for in depth dose analysis. Use micro-CT images to construct a voxel phantom model, apply MCNP to calculate absorbed fraction and dose conversion factor, study the impact in environmental dosimetry are three main steps of the study. However, given the size of larvae and layer of beeswax wall, the absorbed dose fractions show that electrons and photons escaped as the energy increased. For the photons, the energy deposition in source organ decreases to a quasi-threshold value, where no additional energy is deposited as the energy of incident photons increase. The low energy photon is mostly attributed to photoelectric absorption mechanism. This also illustrated that photons are just simply pass the material without interaction. For the electrons, there is decreasing absorbed fraction with target material on the condition that there is amount of energy absorbed by another organ.

The primary object of this research is to accomplish and explain the significance and relevance of absorbed fraction data for the International Commission of Radiation Protection for Reference Animals and Plans, and gain a useful computer model of a beehive, was achieved and can be carried on and used to further the understanding of radiation interactions with beehives. This model could be of great value to consider radionuclide contamination and calculate dose to juvenile bees. It is necessary to model the juvenile bees within the comb receiving the dose from the honey that surrounds

them. The data provided by this study will be used with environmental concentration data to assess the varying exposure situations. Further research could be adding more objects, such as honey and royal jelly to beehive, incorporating the travel of bees throughout the hive and environment. The fundamental model is used to generate absorbed fractions, which are sequentially used to calculate dose conversion factor from radionuclides that uniformly distributed over the organism. These creation models provide better assessment of radiological impacts on the environment.

## Reference

Able Software Corp. (2008). *3D-DOCTOR User's Manual*, Lexington, MA

Bréchnignac, F. (2001). Impact of radioactivity on the environment: Problems, state of current knowledge and approaches for identification of radioprotection criteria. *Radioprotection*, 36(4), 511-535.

Elemental Combustion System - Costech. (n.d.). Retrieved February 12, 2017, from <http://www.bing.com/cr?IG=63C417D6A0134D2BBEA5C076F2CE579D&CID=3CC0EA5B435A6E591FA7E07C426B6FCA&rd=1&h=sA4-JNtoyUi7agltvdfgFyeUKJEtX5XVQJYkuOX9BqQ&v=1&r=http%3a%2f%2fcostechanalytical.com%2fdocumentation%2fECS%25204010%2520Brochure.pdf&p=DevEx,5079.1>

Davenport, K. (2008). *Natural Healing & Me 2*. Oklahoma City, OK.

Devillers, J. (2002). The ecological importance of honey bees and their relevance to ecotoxicology. *Honey Bees*, 1-11.

Griffiths, H. J. (1989). Tissue Substitutes in Radiation Dosimetry and Measurement. No. 4. *Radiology*, 173(1), 202-202.

Gomez, M. F. (2016). Creation and Application of Voxelized Dosimetric Models: An Evaluation of Elemental Sensitivity in Dose Conversion Factors in *Apis Mellifera*.

Haarmann, T. K. (1998). Honey Bees as Indicators of Radionuclide Contamination: Comparative Studies of Contaminant Levels in Forager and Nurse Bees and in the Flowers of Three Plant Species. *Archives of Environmental Contamination and Toxicology*, 35(2), 287-294.

Higley, K., Ruedig, E., Gomez-Fernandez, M., Caffrey, E., Jia, J., Comolli, M., & Hess, C. (2015). Creation and application of voxelised dosimetric models, and a comparison with the current methodology as used for the International Commission on Radiological Protection's Reference Animals and Plants. *Annals of the ICRP*, 44(1\_suppl), 313-330.

Holmes, E. E., Sabo, J. L., Viscido, S. V., & Fagan, W. F. (2007). A statistical approach to quasi-extinction forecasting. *Ecology Letters*, 10(12), 1182-1198.

Hsieh, J. (2009). *Computed tomography: principles, design, artifacts, and recent advances* (2nd ed.). Bellingham, WA. doi:SPIE-The International Society for Optical Engineering

ICRP, (2007). The 2007 Recommendations of the International Commission on Radiological Protection. ICRP Publication 103. *Annals of the ICRP*, 37(2-4).

ICRP, (2008). Environmental Protection: The Concept and Use of Reference Animals and Plants. ICRP Publication 108. *Annals of the ICRP*, 38(4-6).

ICRP, (2010). ICRP Committee 5. Available at: [http://www.icrp.org/icrp\\_group.asp?id=12](http://www.icrp.org/icrp_group.asp?id=12). Issues Related to the use of MCNP code for an extremely large voxel model

Kramer, G. H., Capello, K., Chiang, A., Cardenas-Mendez, E., & Sabourin, T. (2010). Tools For Creating And Manipulating Voxel Phantoms. *Health Physics*, 98(3), 542-548.

Loevinger, R. & Berman, M. (1976). A Revised Schema for Calculating the Absorbed Dose from Biologically Distributed Radionuclides.pdf, New York: Society of Nuclear Medicine.

Los Alamos National Laboratory (2003). Volume I: MCNP Overview and Theory. Oak Ridge, TN: Department of Energy

Los Alamos National Laboratory (2003). Volume II: MCNP User's Guide. Oak Ridge, TN: Department of Energy

Los Alamos National Laboratory (2006). MCNP6.1/MCNP5/MCNPX [computer software]. Oak Ridge, TN.

McHugh, M. L. (2008). Standard error: meaning and interpretation. *Biochemia Medica* 18(1):7-13. School of Nursing, University of Indianapolis, Indianapolis, Indiana, USA.

Murty, R. C. (1965). Effective Atomic Numbers of Heterogeneous Materials. *Nature*, 207(4995), 398-399.

Pentreath, R. (2009). Radioecology, radiobiology, and radiological protection: frameworks and fractures. *Journal of Environmental Radioactivity*, 100(12), 1019-1026.

Shultis, J.K. & Faw, R.E. (2000). Radiation Shielding 2nd ed., La Grange Park, Illinois: American Nuclear Society.

Singh, V., & Badiger, N. (2014). Effective atomic numbers of some tissue substitutes by different methods: A comparative study. *Journal of Medical Physics*, 39(1), 24.

Snodgrass, R. E. (1956). *Anatomy of the honey bee*. Ithaca, NY: Comstock Pub. Associates.

Stabin, M.G. et al. (2006). Voxel-Based Mouse and Rat Models for Internal Dose Calculations. *Journal of Nuclear Medicine*, 47, 655-659.

Ulanovsky, A., Pröhl, G., & Gómez-Ros, J. (2008). Methods for calculating dose conversion coefficients for terrestrial and aquatic biota. *Journal of Environmental Radioactivity*, 99(9), 1440-1448.

Ultra-Micro Balance Sartorius SE2. (n.d.). Retrieved February 12, 2017, from <http://scaleman.com/sartorius-se2-ultra-micro-balance.html>

United States Department of Energy: Nevada Operations Office. (2000). United States Nuclear Tests: July 1945 through September 1992 (DOE/NV 209-REV-15). Springfield, VA: United States Department of Commerce: National Technology Information Service

Winston, M. L. (1987). *The biology of the honey bee*. Cambridge, MA: Harvard University Press.

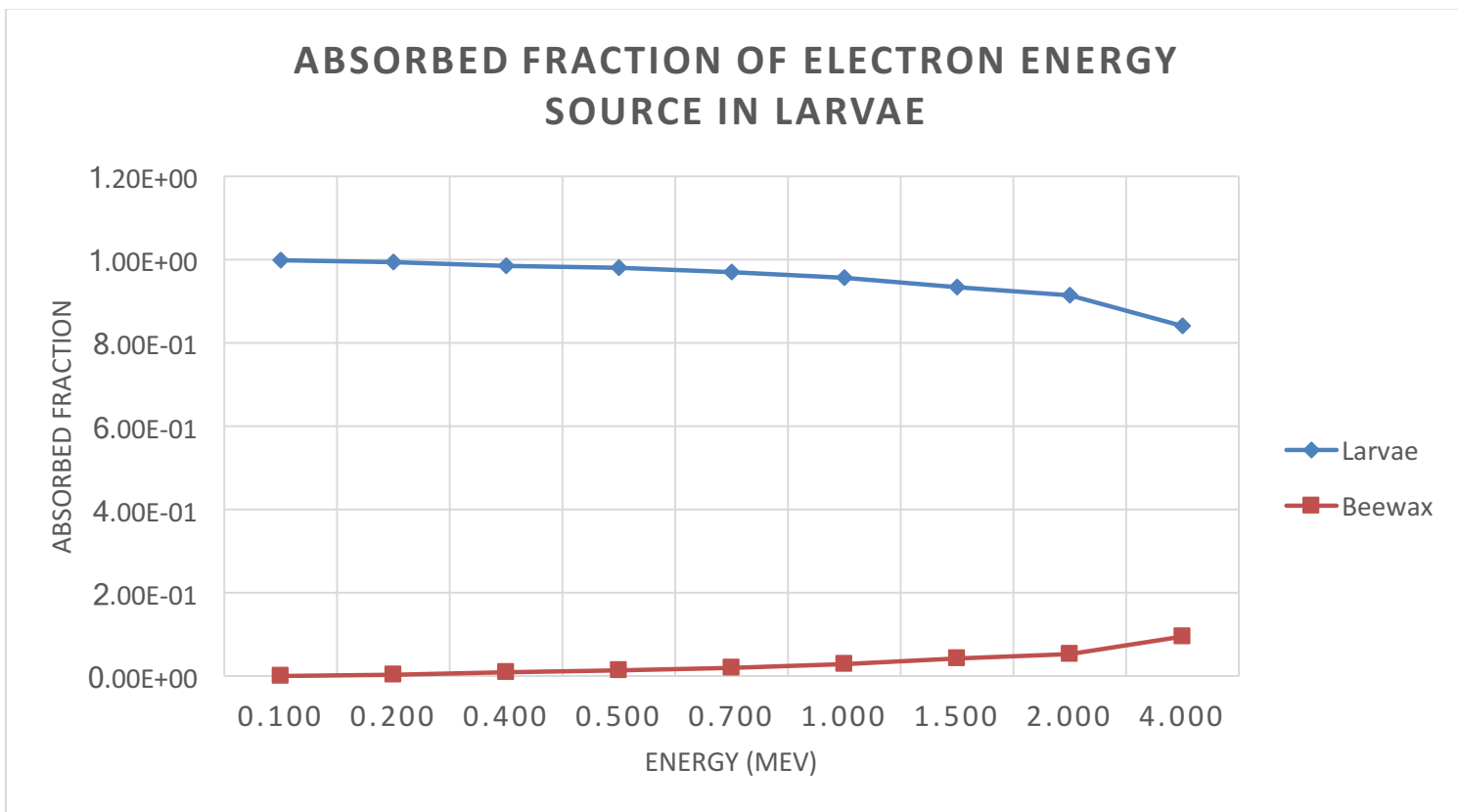
Zaidi, H., & Xu, X. G. (2007). Computational Anthropomorphic Models of the Human Anatomy: The Path to Realistic Monte Carlo Modeling in Radiological Sciences. *Annual Review of Biomedical Engineering*, 9(1), 471-500.

## APPENDICES

## A. Absorbed Fractions of Electron Energy Using Larvae Tissue Composition

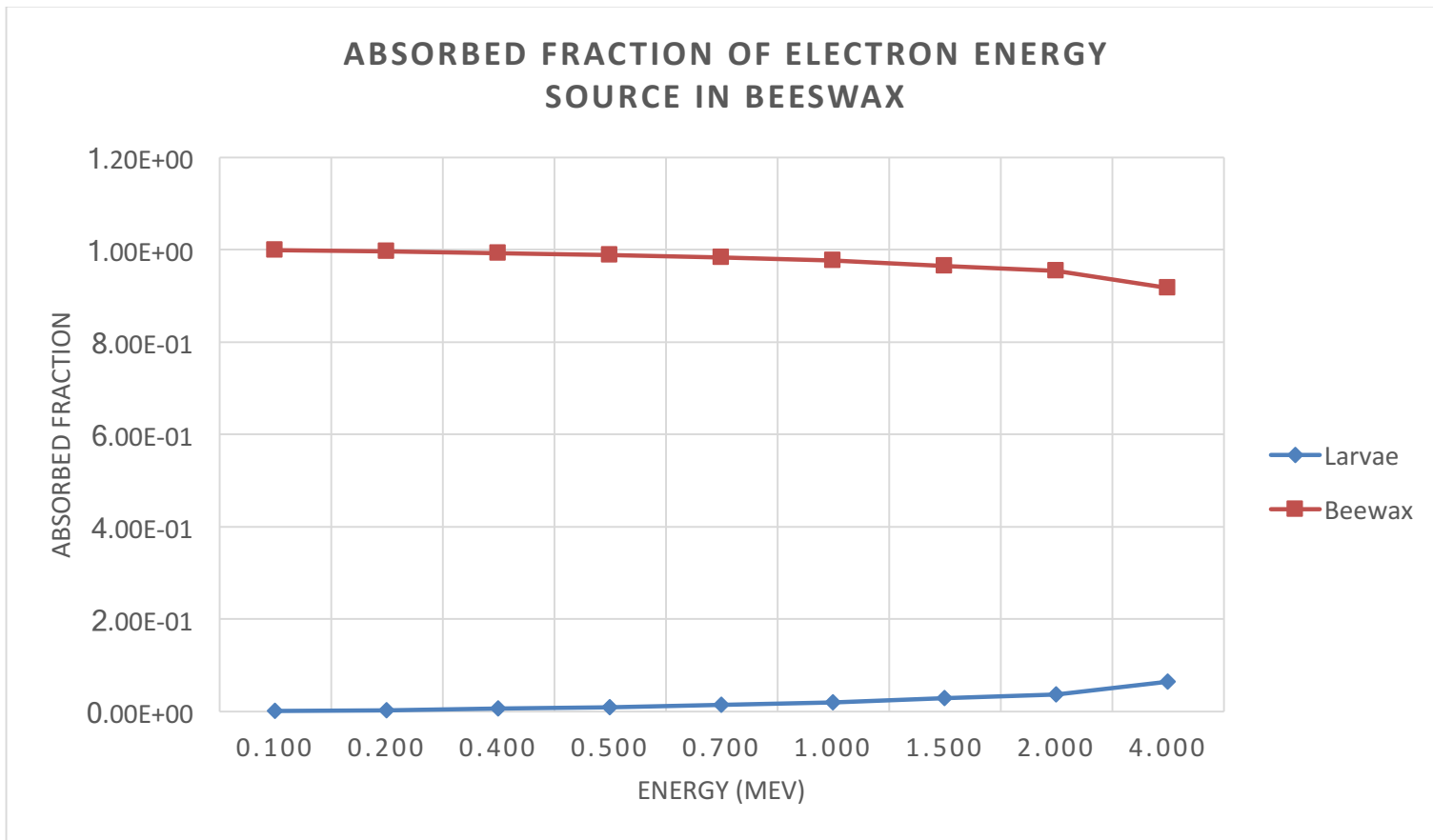
ABSORBED FRACTIONS OF ELECTRON ENERGY

	Source in Larvae								
	Energy (MeV)								
TARGET	0.100	0.200	0.400	0.500	0.700	1.000	1.500	2.000	4.000
<b>LARVAE</b>	9.98E-02	1.99E-01	3.94E-01	4.90E-01	6.79E-01	9.56E-01	1.40E+00	1.83E+00	3.37E+00
<b>BEESWAX</b>	1.20E-04	7.56E-04	4.09E-03	6.80E-03	1.42E-02	2.91E-02	6.35E-02	1.08E-01	3.78E-01



ABSORBED FRACTIONS OF ELECTRON ENERGY

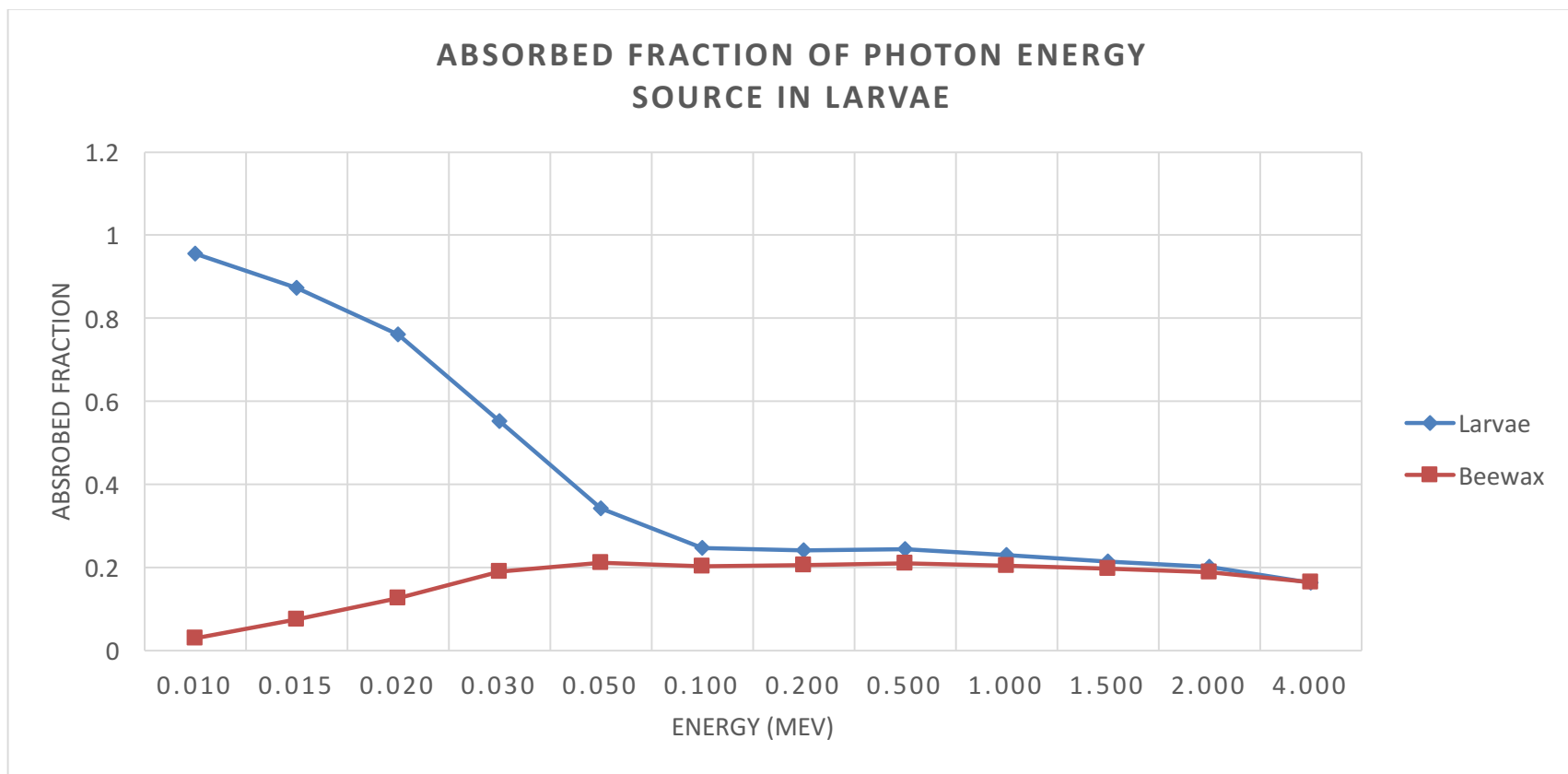
	Source in Beeswax Energy (MeV)								
TARGET	0.100	0.200	0.400	0.500	0.700	1.000	1.500	2.000	4.000
<b>LARVAE</b>	7.61E-05	4.99E-04	2.73E-03	4.57E-03	9.53E-03	1.98E-02	4.29E-02	7.31E-02	2.57E-01
<b>BEESWAX</b>	9.99E-02	1.99E-01	3.97E-01	4.95E-01	6.89E-01	9.76E-01	1.45E+00	1.91E+00	3.67E+00



## B. Absorbed Fractions of Photon Energy Using Larvae Tissue Composition

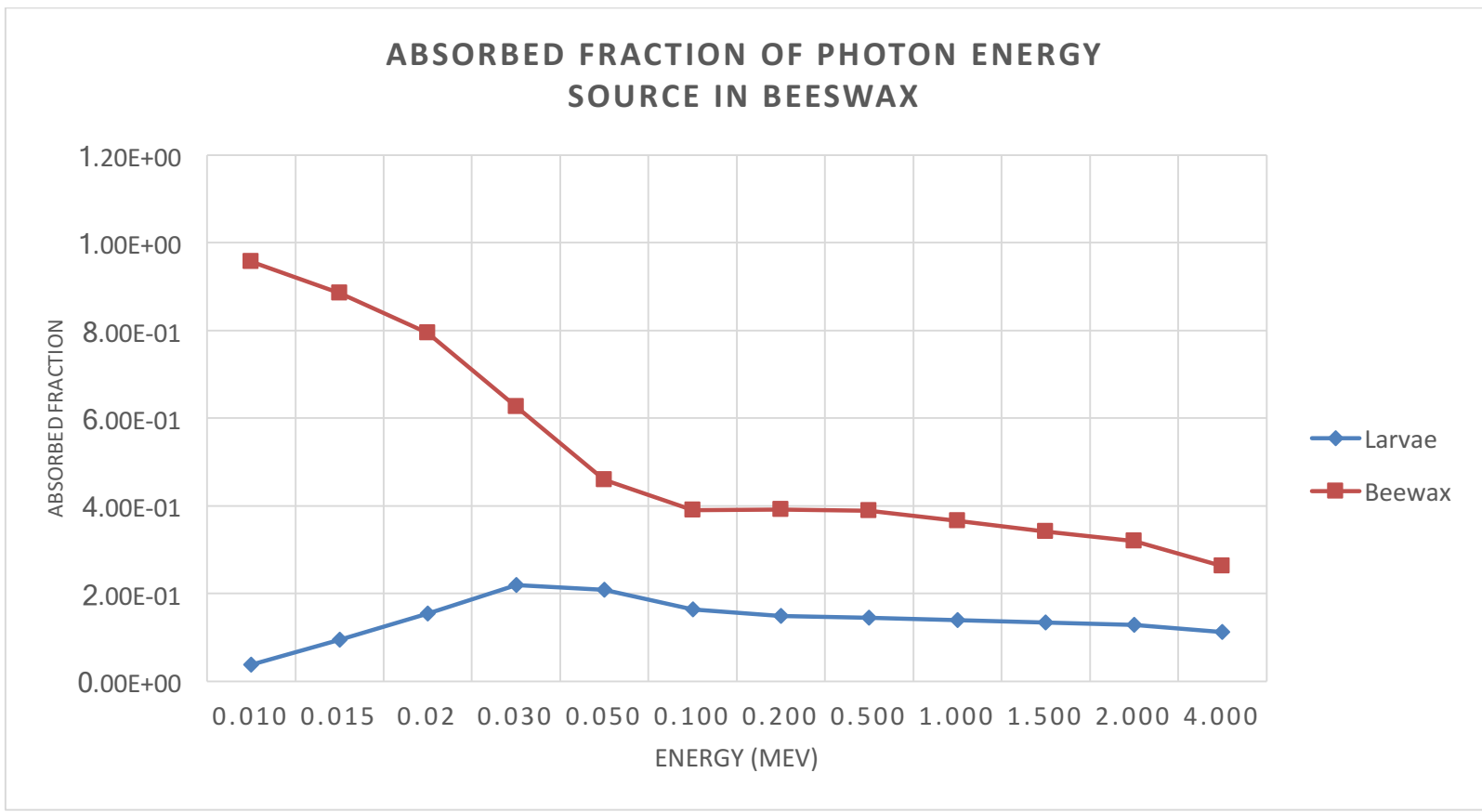
ABSORBED FRACTIONS OF PHOTON ENERGY

	Source in Larvae											
	Energy (MeV)											
TARGET	0.010	0.015	0.020	0.030	0.050	0.100	0.200	0.500	1.000	1.500	2.000	4.000
<b>LARVAE</b>	9.55E-03	1.31E-02	1.52E-02	1.66E-02	1.71E-02	2.47E-02	4.83E-02	1.22E-01	2.30E-01	3.21E-01	4.01E-01	6.50E-01
<b>BEESWAX</b>	2.98E-04	1.13E-03	2.51E-03	5.69E-03	1.05E-02	2.03E-02	4.11E-02	1.05E-01	2.04E-01	2.95E-01	3.78E-01	6.58E-01



ABSORBED FRACTIONS OF PHOTON ENERGY

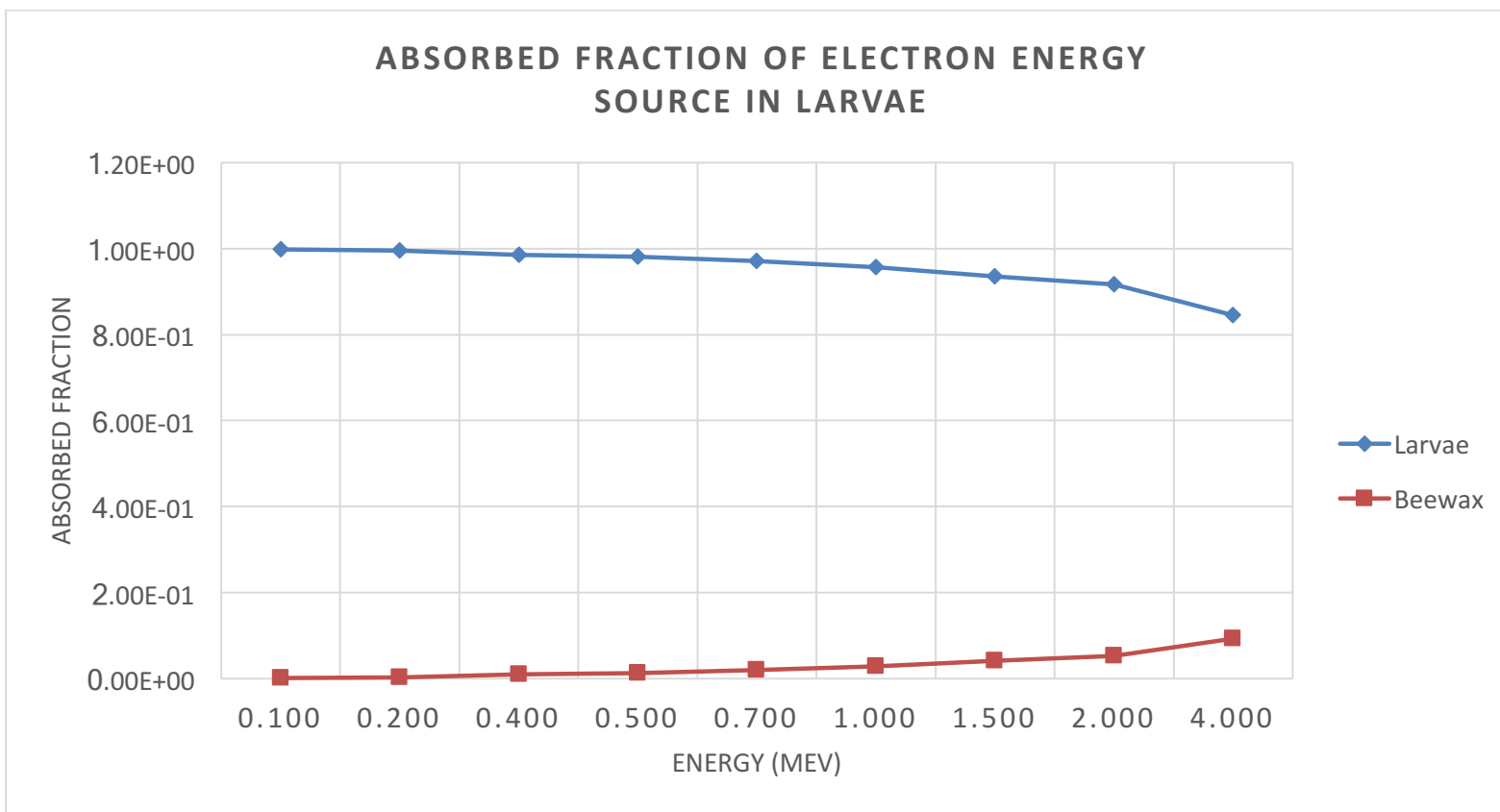
	Source in Beeswax											
	Energy (MeV)											
TARGET	0.010	0.015	0.02	0.030	0.050	0.100	0.200	0.500	1.000	1.500	2.000	4.000
LARVAE	3.72E-04	1.41E-03	3.08E-03	6.56E-03	1.04E-02	1.64E-02	2.97E-02	7.23E-02	1.40E-01	2.01E-01	2.57E-01	4.50E-01
BEESWAX	9.57E-03	1.33E-02	1.59E-02	1.88E-02	2.30E-02	3.90E-02	7.82E-02	1.95E-01	3.66E-01	5.12E-01	6.40E-01	1.05E+00



### C. Absorbed Fractions of Electron Energy Using ICRU Four-Component Human Soft Tissue

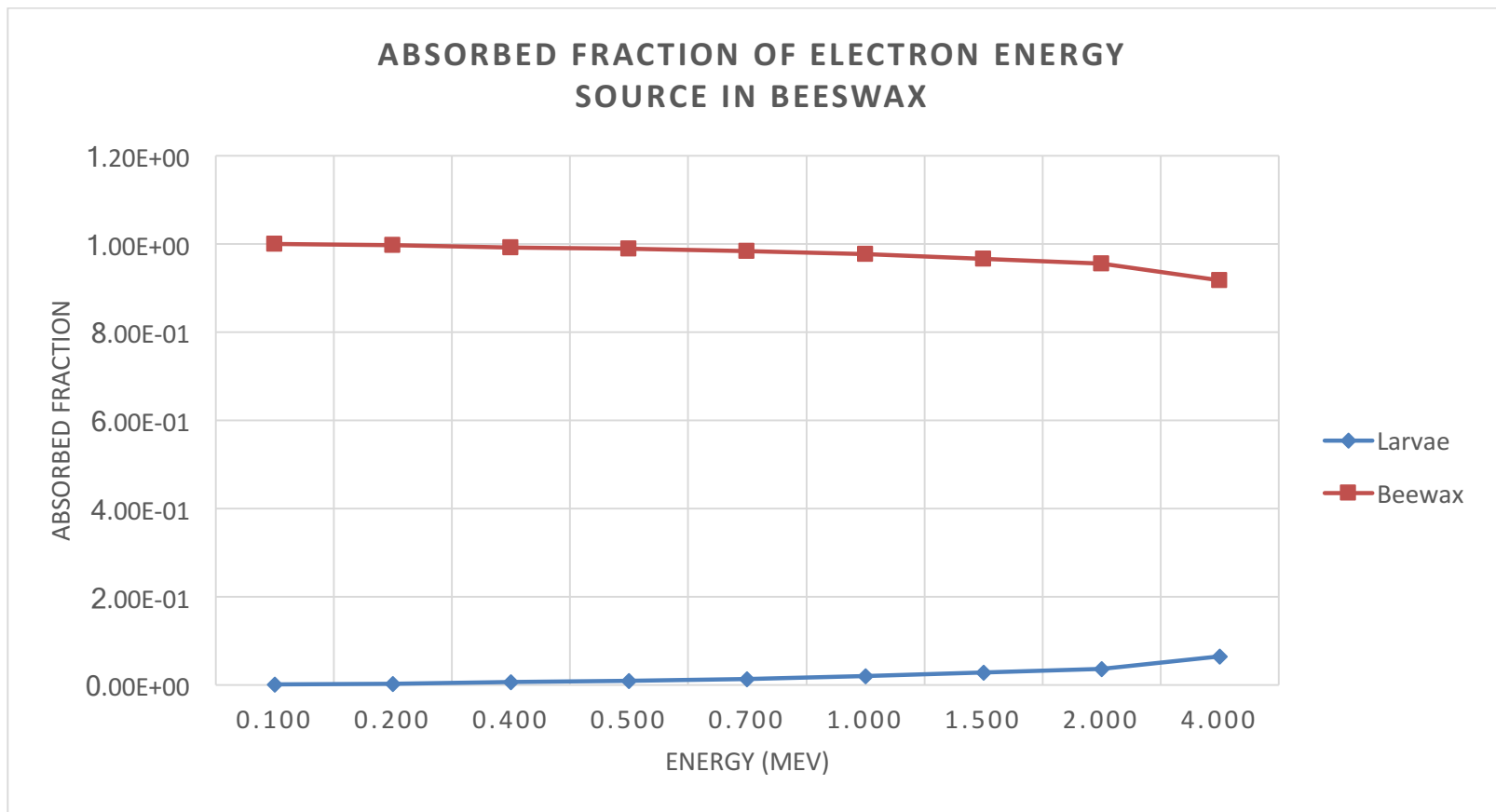
ABSORBED FRACTIONS OF ELECTRON ENERGY

	Source in Larvae								
	Energy (MeV)								
TARGET	0.100	0.200	0.400	0.500	0.700	1.000	1.500	2.000	4.000
LARVAE (H)	9.98E-02	1.99E-01	3.94E-01	4.90E-01	6.80E-01	9.57E-01	1.40E+00	1.83E+00	3.38E+00
BEESWAX	1.14E-04	7.34E-04	3.99E-03	6.62E-03	1.38E-02	2.84E-02	6.19E-02	1.05E-01	3.70E-01



ABSORBED FRACTIONS OF ELECTRON ENERGY

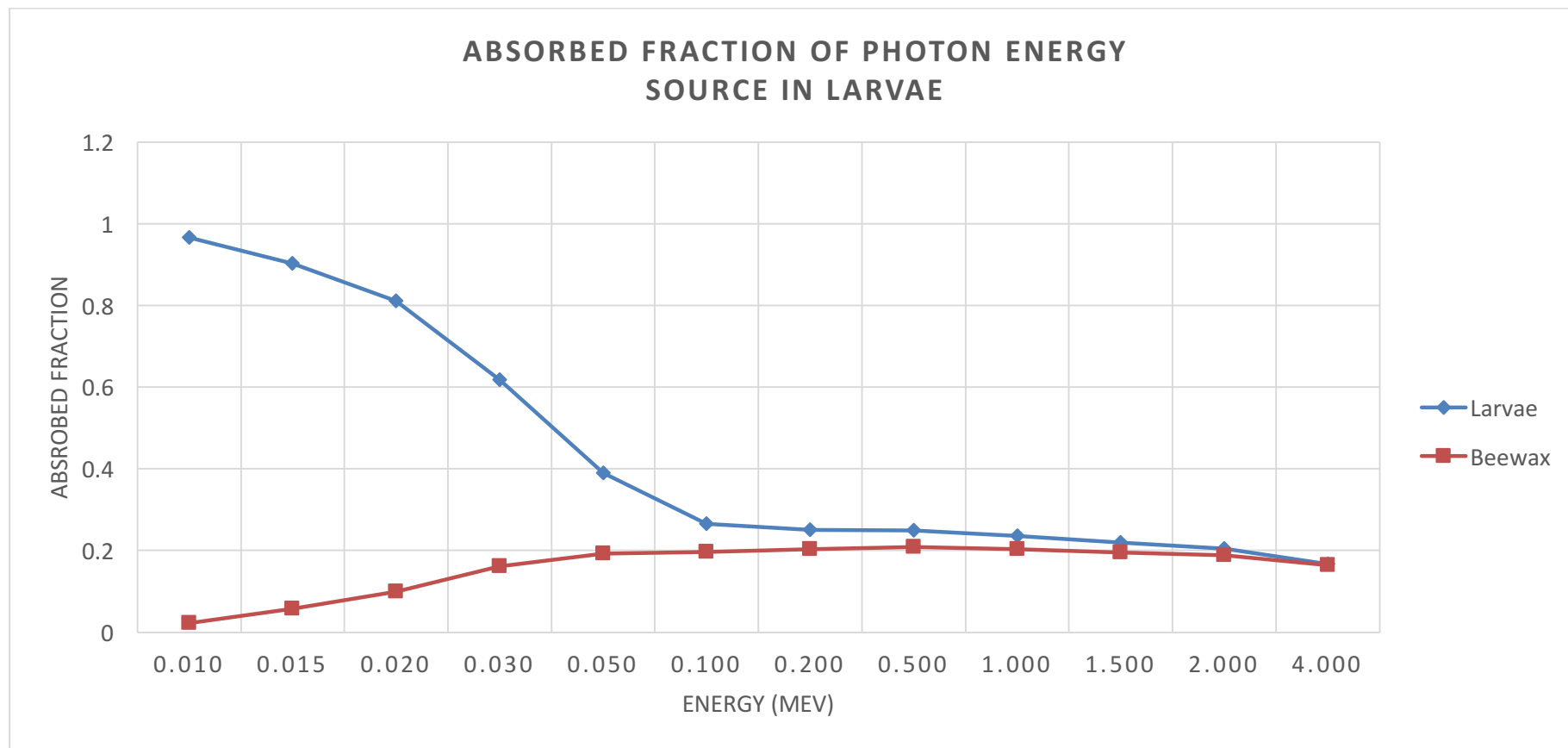
	Source in Beeswax								
	Energy (MeV)								
TARGET	0.100	0.200	0.400	0.500	0.700	1.000	1.500	2.000	4.000
<b>LARVAE (H)</b>	7.63E-05	4.99E-04	2.73E-03	4.56E-03	9.54E-03	1.99E-02	4.30E-02	7.33E-02	2.58E-01
<b>BEESWAX</b>	9.99E-02	1.99E-01	3.97E-01	4.95E-01	6.89E-01	9.76E-01	1.45E+00	1.91E+00	3.67E+00



### D. Absorbed Fractions of Photon Energy Using ICRU Four-Component Human Soft Tissue

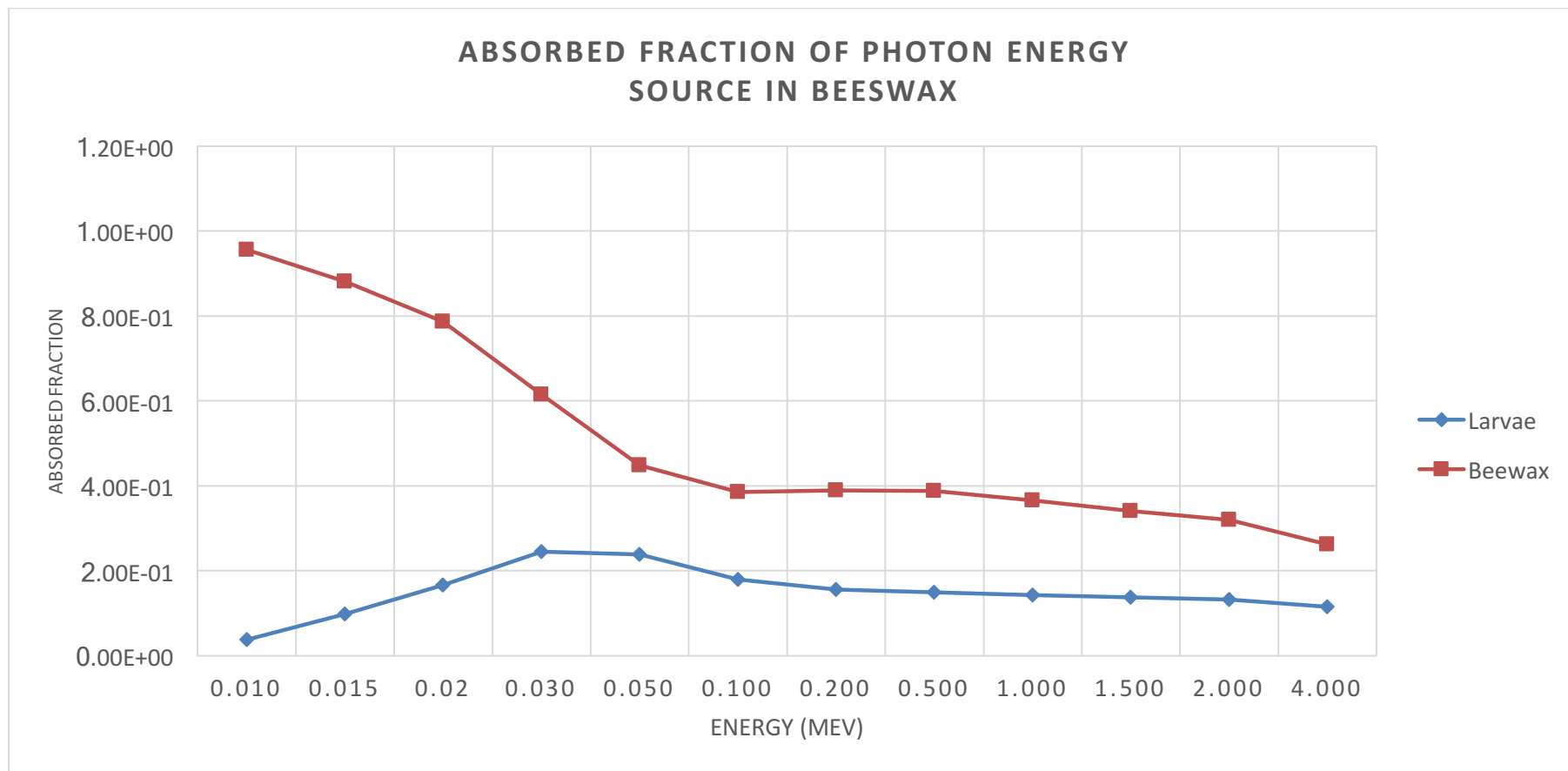
ABSORBED FRACTIONS OF PHOTON ENERGY

	Source in Larvae											
	Energy (MeV)											
TARGET	0.010	0.015	0.020	0.030	0.050	0.100	0.200	0.500	1.000	1.500	2.000	4.000
<b>LARVAE (H)</b>	9.66E-03	1.35E-02	1.62E-02	1.85E-02	1.95E-02	2.66E-02	5.01E-02	1.25E-01	2.35E-01	3.28E-01	4.10E-01	6.67E-01
<b>BEESWAX</b>	2.27E-04	8.73E-04	1.99E-03	4.82E-03	9.65E-03	1.97E-02	4.06E-02	1.04E-01	2.03E-01	2.93E-01	3.76E-01	6.56E-01



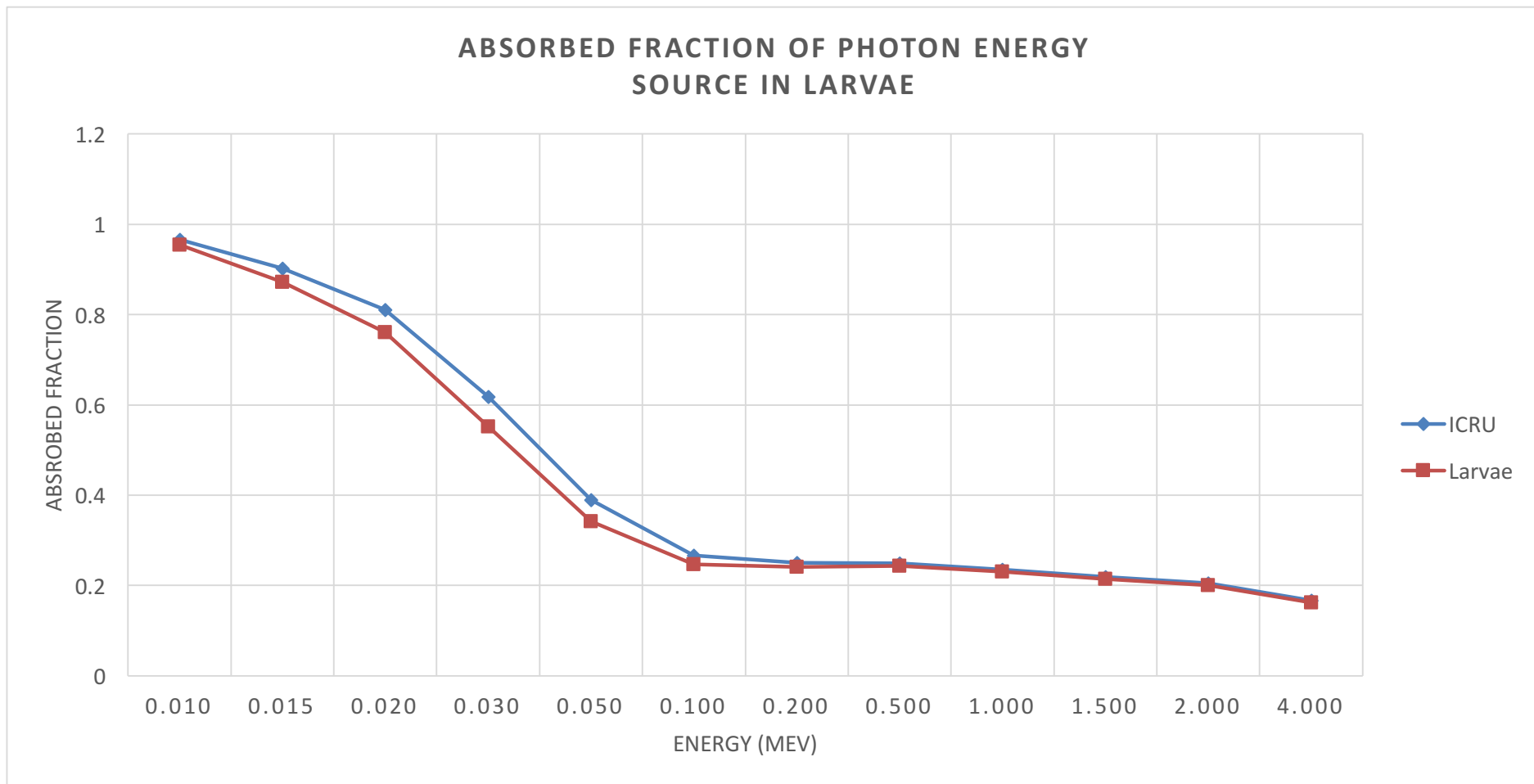
ABSORBED FRACTIONS OF PHOTON ENERGY

TARGET	Source in Beeswax											
	Energy (MeV)											
	0.010	0.015	0.02	0.030	0.050	0.100	0.200	0.500	1.000	1.500	2.000	4.000
<b>LARVAE (H)</b>	3.83E-04	1.48E-03	3.31E-03	7.36E-03	1.19E-02	1.79E-02	3.12E-02	7.44E-02	1.43E-01	2.06E-01	2.63E-01	4.62E-01
<b>BEESWAX</b>	9.56E-03	1.32E-02	1.57E-02	1.84E-02	2.24E-02	3.85E-02	7.78E-02	1.94E-01	3.65E-01	5.11E-01	6.39E-01	1.05E+00



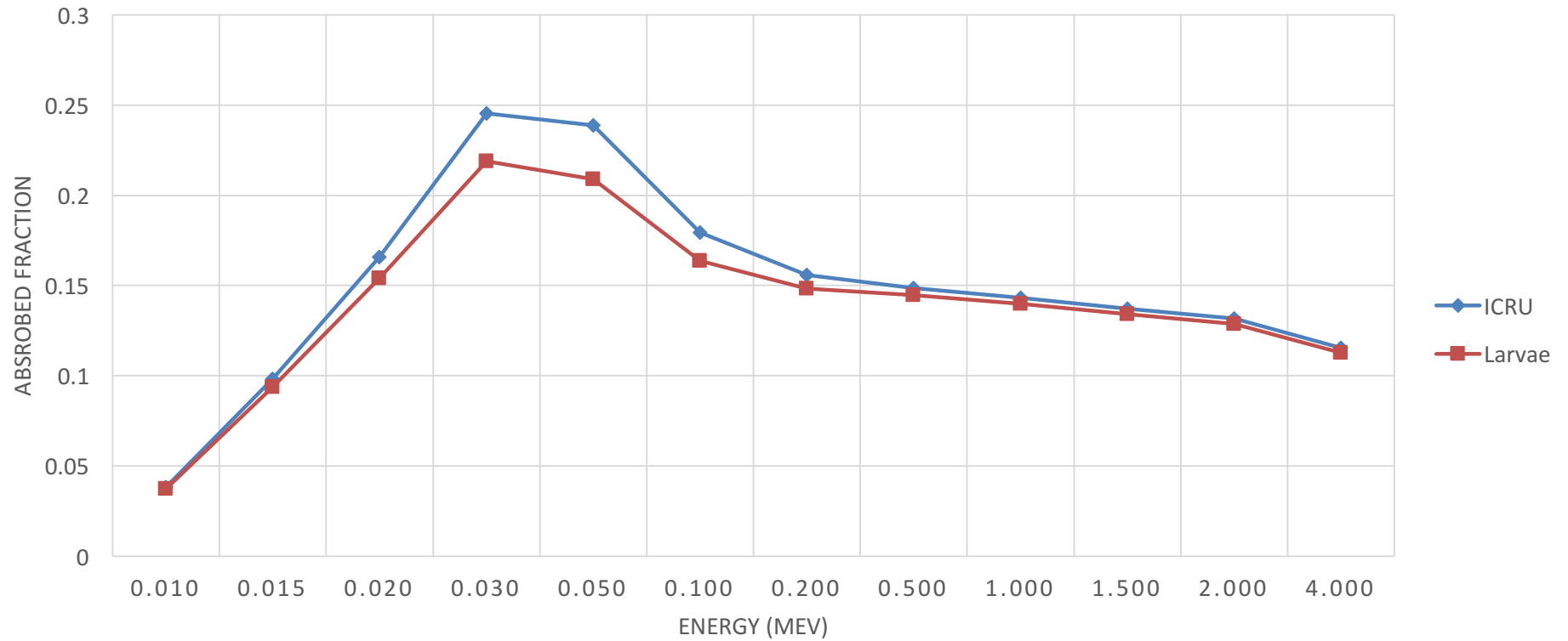
## E. Differentiation of Absorbed Fraction of Photon Energy

ENERGY	0.010	0.015	0.020	0.030	0.050	0.100	0.200	0.500	1.000	1.500	2.000	4.000
<b>ABSORBED FRACTIONS</b>												
<b>ICRU</b>	9.66E-01	9.02E-01	8.11E-01	6.18E-01	3.90E-01	2.66E-01	2.51E-01	2.49E-01	2.35E-01	2.19E-01	2.05E-01	1.67E-01
<b>LARVAE</b>	9.55E-01	8.72E-01	7.61E-01	5.52E-01	3.42E-01	2.47E-01	2.41E-01	2.44E-01	2.30E-01	2.14E-01	2.00E-01	1.63E-01



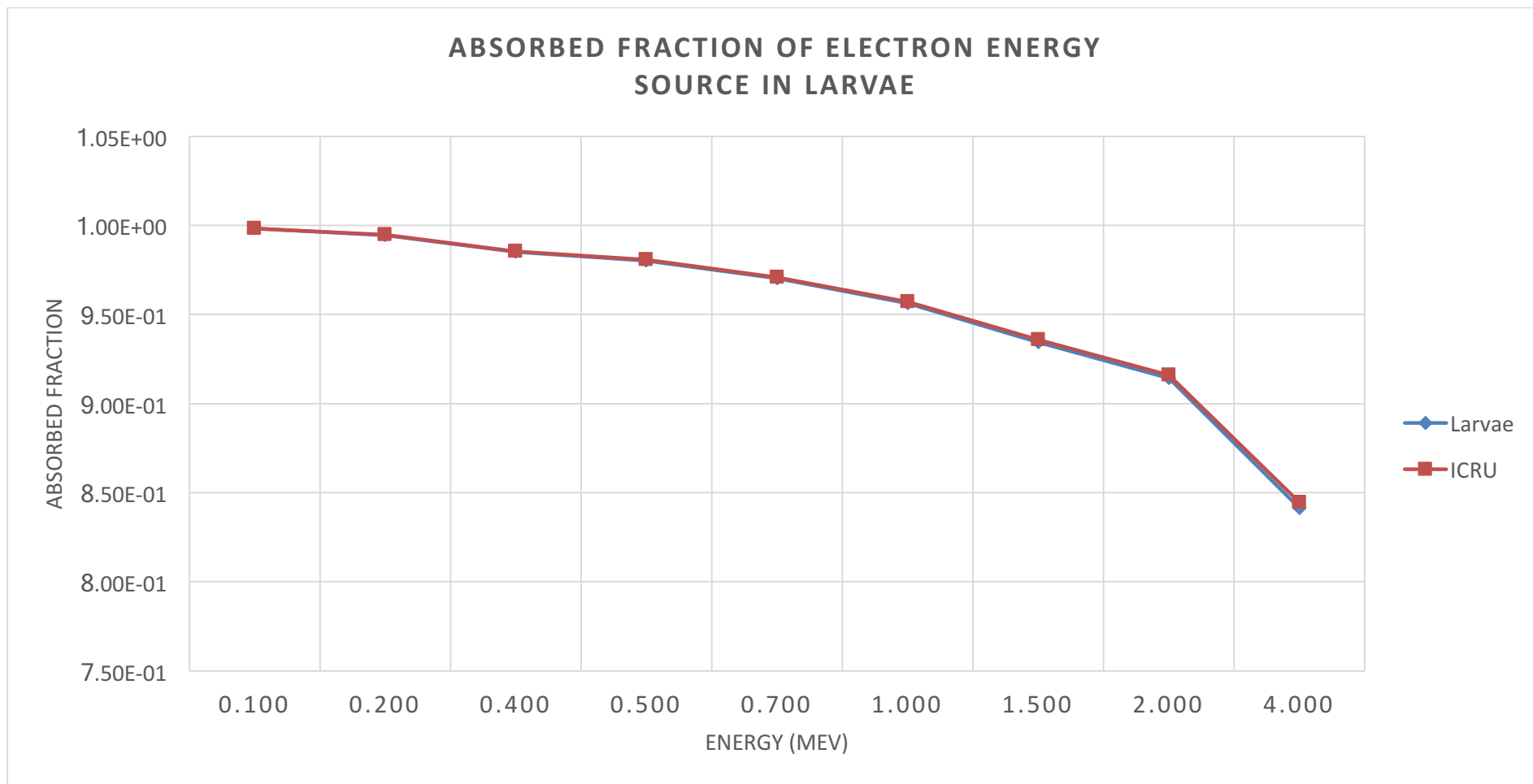
ABSORBED FRACTIONS	0.010	0.015	0.020	0.030	0.050	0.100	0.200	0.500	1.000	1.500	2.000	4.000
ICRU	3.83E-02	9.84E-02	1.66E-01	2.45E-01	2.39E-01	1.79E-01	1.56E-01	1.49E-01	1.43E-01	1.37E-01	1.32E-01	1.15E-01
LARVAE	3.72E-02	9.39E-02	1.54E-01	2.19E-01	2.09E-01	1.64E-01	1.48E-01	1.45E-01	1.40E-01	1.34E-01	1.29E-01	1.13E-01

ABSORBED FRACTION OF PHOTON ENERGY  
SOURCE IN BEESWAX

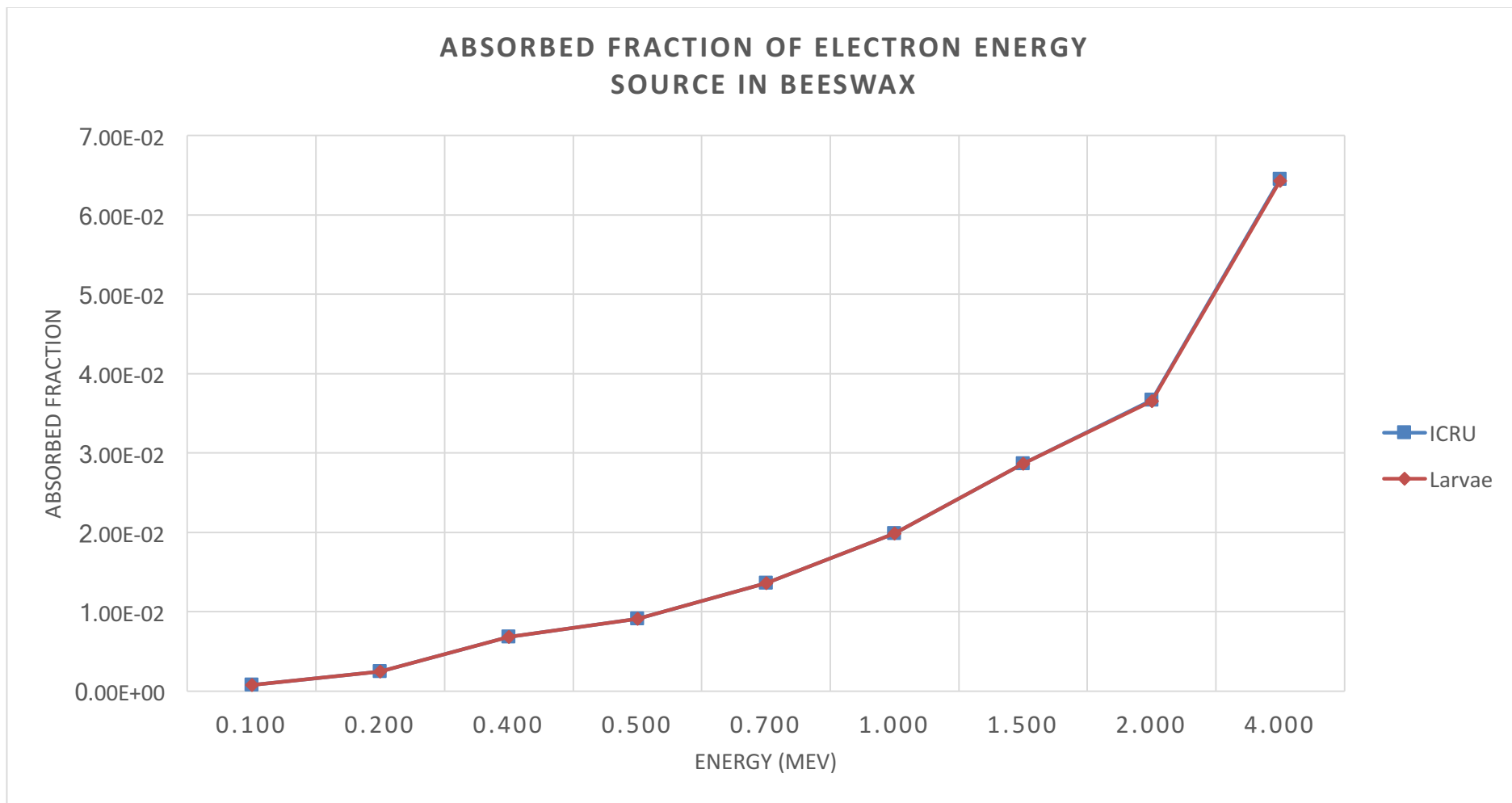


## F. Differentiation of Absorbed Fraction of Electron Energy

ENERGY	0.100	0.200	0.400	0.500	0.700	1.000	1.500	2.000	4.000
<b>ABSORBED FRACTIONS</b>									
<b>ICRU</b>	9.98E-01	9.95E-01	9.86E-01	9.81E-01	9.71E-01	9.57E-01	9.36E-01	9.16E-01	8.44E-01
<b>LARVAE</b>	9.98E-01	9.95E-01	9.85E-01	9.80E-01	9.70E-01	9.56E-01	9.34E-01	9.14E-01	8.41E-01



ENERGY	0.100	0.200	0.400	0.500	0.700	1.000	1.500	2.000	4.000
<b>ABSORBED FRACTIONS ICRU</b>	7.63E-04	2.50E-03	6.84E-03	9.12E-03	1.36E-02	1.99E-02	2.87E-02	3.66E-02	6.44E-02
<b>LARVAE</b>	7.61E-04	2.49E-03	6.83E-03	9.15E-03	1.36E-02	1.98E-02	2.86E-02	3.66E-02	6.43E-02



## G. Organic Elemental Analysis for Bee Larvae

The results of the elemental analysis are provided for larvae tissues, where can be utilized in the input file of MCNP general transport code. The oxygen content is calculated by weight difference between the dried sample and the analyzed sample.

Position	Sample Amount (mg)	Area [mV.s] Nitrogen	Area [mV.s] Carbon	Area [mV.s] Hydrogen	Weight [mg] Nitrogen	Weight [mg] Carbon	Weight [mg] Hydrogen	Weight [%] Nitrogen	Weight [%] Carbon	Weight [%] Hydrogen
A1	1.561	54.214	1177.607	604.61	0.096	0.762	0.115	6.15	48.81	7.39
B1	0.707	20.659	561.681	285.565	0.037	0.361	0.055	5.21	51.05	7.82
C1	0.872	28.925	664.414	347.043	0.051	0.428	0.067	5.9	49.06	7.67
D1	1.06	34.665	792.261	406.275	0.062	0.511	0.078	5.81	48.21	7.36
E1	1.18	37.514	876.699	431.715	0.067	0.566	0.083	5.64	47.97	7.02
F1	0.584	19.157	463.916	234.811	0.034	0.297	0.046	5.86	50.9	7.83
A2	0.891	27.316	707.29	347.676	0.049	0.456	0.067	5.45	51.15	7.52
B2	0.478	15.929	367.447	185.089	0.029	0.234	0.036	5.96	49.04	7.61
C2	1.523	48.881	1179.924	600.284	0.087	0.763	0.115	5.69	50.13	7.52
D2	1.29	39.313	980.038	504.854	0.07	0.633	0.097	5.41	49.1	7.49
E2	0.879	28.893	670.513	329.091	0.051	0.432	0.063	5.85	49.12	7.22
F2	1.03	46.314	773.552	389.624	0.082	0.499	0.075	7.97	48.43	7.27

Position	Sample Amount (mg)	Area [mV.s]	Area [mV.s]	Area [mV.s]	Weight [mg]	Weight [mg]	Weight [mg]	Weight [%]	Weight [%]	Weight [%]
		Nitrogen	Carbon	Hydrogen	Nitrogen	Carbon	Hydrogen	Nitrogen	Carbon	Hydrogen
A1	0.996	25.951	711.391	377.602	0.047	0.47	0.075	4.76	47.2	7.52
A2	0.548	14.108	414.116	217.343	0.026	0.27	0.042	4.66	49.32	7.72
B1	0.894	23.439	672.154	353.588	0.043	0.444	0.07	4.78	49.63	7.83
B2	0.537	12.926	400.109	209.096	0.023	0.261	0.041	4.35	48.58	7.57
C1	0.602	14.301	457.462	227.922	0.026	0.299	0.044	4.3	49.74	7.39
C2	0.638	16.659	461.101	232.651	0.03	0.302	0.045	4.74	47.31	7.12
D1	0.888	21.66	654.006	331.482	0.039	0.432	0.066	4.44	48.6	7.38
D2	0.999	25.295	737.451	385.094	0.046	0.488	0.076	4.62	48.81	7.65
E1	0.81	23.584	587.049	300.077	0.043	0.387	0.059	5.31	47.72	7.3
E2	0.767	25.965	556.861	271.499	0.047	0.366	0.053	6.18	47.75	6.95
F1	0.721	18.346	527.846	263.239	0.033	0.347	0.052	4.62	48.09	7.16
F2	0.826	24.41	597.362	299.59	0.045	0.393	0.059	5.39	47.63	7.15

<b>Average</b>	<b>4.85</b>	<b>48.37</b>	<b>7.40</b>
<b>S.D.</b>	<b>0.54</b>	<b>0.88</b>	<b>0.27</b>
<b>Std Error</b>	<b>0.15</b>	<b>0.25</b>	<b>0.08</b>
<b>Max</b>	<b>6.18</b>	<b>49.74</b>	<b>7.83</b>
<b>Min</b>	<b>4.30</b>	<b>47.20</b>	<b>6.95</b>
<b>Median</b>	<b>4.66</b>	<b>48.58</b>	<b>7.39</b>

Number of samples 24.000

seems a bit of an outlier... maybe consider excluding?

### H. MCNP Input Code with Source in Bee Larvae: Photon

The following code is a sample of MCNP inputs, and there are three data needed to be changed when run code in different situation: erg, si4 and par (This code is not a completed due to lattice unit cell have a thousand papers).

```
c This input file was made with the MCNP Lattice Tool
c originally created by Erick Daniel Cardenas-Mendez (a.k.a. Ace Wave)
c for the Human Monitoring Laboratory of Health Canada
c
c Input file originally created on:
c Thu Aug 6 2015
c
c Empty space universe: 3
c compression factor: 5
c
c
c
c ++++++
c
c Cells
c
c ++++++
c
999 0 999                imp:p 0 imp:e 0    $ outside
998 3 -.1205E-02 -999 1111 #997    imp:p 1 imp:e 1    $ air
```

c

c Filling Universes

```
1 1 -1.0000 -2222 u = 1 imp:p 1 imp:e 1 $Larvae
100 0 2222 u = 1 imp:p 0 imp:e 0 $Larvae
2 2 -1.0000 -2222 u = 2 imp:p 1 imp:e 1 $Wall
200 0 2222 u = 2 imp:p 0 imp:e 0 $Wall
3 3 -.120E-02 -2222 u = 3 imp:p 1 imp:e 1 $Surrounding Air
300 0 2222 u = 3 imp:p 0 imp:e 0 $Surrounding Air
```

c

c Lattice Unit Cell

c

```
996 0 -2222 lat = 1 u = 996 imp:p 1 imp:e 1
fill = 0:405 0:407 0:301
3 43449r 1 1r 3 404r 1 2r 3 403r 1 3r 3 401r 1 5r 3 399r 1 9r 3
395r 1 12r 3 392r 1 15r 3 389r 1 18r 3 1 1r 3 1 3 380r 1 30r 3
374r 1 34r 3 370r 1 38r 3 366r 1 41r 3 310r 1 3 51r 1 44r 3
306r 1 3r 3 49r 1 47r 3 1 1r 3 301r 1 4r 3 46r 1 51r 3 302r 1
6r 3 43r 1 52r 3 301r 1 10r 3 39r 1 53r 3 301r 1 12r 3 35r 1
56r 3 299r 1 15r 3 32r 1 57r 3 297r 1 19r 3 29r 1 59r 3 295r 1
23r 3 24r 1 25r 2 12r 1 22r 3 293r 1 30r 3 18r 1 23r 2 16r 1
21r 3 292r 1 33r 3 15r 1 23r 2 19r 1 19r 3 291r 1 38r 3 10r 1
23r 2 21r 1 18r 3 290r 1 41r 3 7r 1 14r 2 4r 1 3r 2 23r 1 17r 3
289r 1 45r 3 1 17r 2 6r 1 1r 2 25r 1 17r 3 287r 1 64r 2 7r 1
1r 2 26r 1 16r 3 236r 1 3 47r 1 19r 2 1 46r 2 5r 1 1r 2 28r 1
15r 3 236r 1 3 46r 1 14r 2 12r 1 48r 2 29r 1 14r 3 236r 1 1r 3
```

44r 1 12r 2 17r 1 43r 2 33r 1 14r 3 234r 1 3r 3 42r 1 12r 2  
20r 1 40r 2 34r 1 14r 3 234r 1 6r 3 39r 1 10r 2 24r 1 38r 2  
35r 1 13r 3 233r 1 11r 3 33r 1 11r 2 26r 1 37r 2 36r 1 12r 3  
231r 1 17r 3 28r 1 11r 2 28r 1 36r 2 36r 1 13r 3 229r 1 20r 3  
25r 1 12r 2 29r 1 36r 2 35r 1 13r 3 228r 1 24r 3 21r 1 12r 2  
31r 1 35r 2 35r 1 13r 3 227r 1 28r 3 17r 1 13r 2 31r 1 37r 2  
33r 1 13r 3 226r 1 31r 3 14r 1 9r 2 2r 1 2 33r 1 36r 2 33r 1  
14r 3 224r 1 35r 3 10r 1 9r 2 38r 1 36r 2 33r 1 14r 3 222r 1  
38r 3 8r 1 10r 2 38r 1 32r 2 37r 1 15r 3 220r 1 42r 3 3r 1 12r 2  
39r 1 31r 2 37r 1 15r 3 219r 1 60r 2 39r 1 31r 2 37r 1 15r 3  
165r 1 1r 3 50r 1 65r 2 34r 1 34r 2 35r 1 15r 3 165r 1 1r 3  
48r 1 67r 2 34r 1 35r 2 35r 1 14r 3 165r 1 2r 3 1 1r 3 43r 1  
68r 2 34r 1 35r 2 35r 1 14r 3 164r 1 8r 3 40r 1 70r 2 32r 1  
36r 2 35r 1 14r 3 163r 1 11r 3 37r 1 71r 2 31r 1 36r 2 36r 1  
15r 3 161r 1 15r 3 33r 1 72r 2 31r 1 35r 2 37r 1 15r 3 160r 1  
19r 3 29r 1 24r 2 9r 1 38r 2 30r 1 35r 2 37r 1 16r 3 159r 1  
23r 3 25r 1 23r 2 13r 1 35r 2 31r 1 35r 2 37r 1 17r 3 156r 1  
27r 3 22r 1 22r 2 18r 1 31r 2 32r 1 35r 2 36r 1 18r 3 155r 1  
30r 3 18r 1 22r 2 21r 1 30r 2 31r 1 30r 2 3r 1 1r 2 36r 1 18r 3  
154r 1 34r 3 13r 1 23r 2 23r 1 28r 2 32r 1 30r 2 3r 1 1r 2 35r 1  
20r 3 152r 1 37r 3 10r 1 24r 2 25r 1 26r 2 32r 1 30r 2 4r 1  
2 35r 1 20r 3 151r 1 41r 3 7r 1 23r 2 27r 1 26r 2 31r 1 30r 2  
4r 1 2 34r 1 20r 3 150r 1 68r 2 1r 1 4r 2 27r 1 26r 2 31r 1  
31r 2 3r 1 2 34r 1 20r 3 95r 1 3 52r 1 68r 2 4r 1 1r 2 29r 1  
26r 2 30r 1 37r 2 32r 1 17r 3 1 1r 3 96r 1 1r 3 50r 1 8r 2 4r 1

55r 2 4r 1 1r 2 30r 1 25r 2 30r 1 37r 2 31r 1 18r 3 99r 1 4r 3  
45r 1 8r 2 9r 1 52r 2 4r 1 1r 2 30r 1 26r 2 29r 1 38r 2 29r 1  
18r 3 99r 1 8r 3 41r 1 8r 2 12r 1 54r 2 1 1r 2 30r 1 26r 2 29r 1  
39r 2 27r 1 17r 3 100r 1 11r 3 38r 1 8r 2 14r 1 54r 2 1 2 31r 1  
24r 2 30r 1 40r 2 25r 1 17r 3 100r 1 15r 3 33r 1 8r 2 17r 1  
52r 2 2r 1 2 30r 1 19r 2 1r 1 2r 2 30r 1 41r 2 23r 1 17r 3 100r 1  
19r 3 29r 1 8r 2 19r 1 50r 2 4r 1 2 29r 1 19r 2 35r 1 42r 2  
20r 1 18r 3 100r 1 23r 3 24r 1 9r 2 21r 1 50r 2 35r 1 18r 2  
36r 1 44r 2 15r 1 19r 3 100r 1 27r 3 19r 1 3 1 8r 2 22r 1 50r 2  
4r 1 2 29r 1 18r 2 36r 1 47r 2 8r 1 21r 3 101r 1 30r 3 16r 1  
3 1 8r 2 23r 1 50r 2 35r 1 18r 2 37r 1 76r 3 101r 1 13r 2 5r 1  
15r 3 13r 1 7r 2 25r 1 51r 2 34r 1 23r 2 32r 1 75r 3 101r 1  
11r 2 11r 1 16r 3 6r 1 3 1 7r 2 26r 1 52r 2 33r 1 23r 2 32r 1  
74r 3 100r 1 6r 2 2r 1 2r 2 16r 1 16r 3 1 11r 2 25r 1 54r 2  
32r 1 24r 2 31r 1 73r 3 100r 1 6r 2 4r 1 2 19r 1 27r 2 25r 1  
54r 2 32r 1 24r 2 30r 1 72r 3 101r 1 6r 2 27r 1 26r 2 24r 1  
56r 2 31r 1 24r 2 30r 1 71r 3 101r 1 7r 2 29r 1 24r 2 26r 1  
55r 2 30r 1 25r 2 28r 1 71r 3 101r 1 8r 2 30r 1 23r 2 27r 1  
1r 2 4r 1 47r 2 30r 1 26r 2 26r 1 71r 3 100r 1 13r 2 28r 1 23r 2  
27r 1 2 4r 1 47r 2 30r 1 27r 2 24r 1 71r 3 100r 1 14r 2 28r 1  
24r 2 32r 1 47r 2 30r 1 28r 2 21r 1 72r 3 100r 1 15r 2 29r 1  
22r 2 33r 1 39r 2 1r 1 9r 2 26r 1 29r 2 19r 1 71r 3 100r 1 16r 2  
31r 1 19r 2 35r 1 38r 2 1 1r 2 1 9r 2 25r 1 32r 2 14r 1 72r 3  
100r 1 18r 2 30r 1 18r 2 36r 1 38r 2 1r 1 2r 2 1 7r 2 25r 1  
35r 2 7r 1 75r 3 99r 1 20r 2 31r 1 17r 2 35r 1 44r 2 2r 1 4r 2

26r 1 117r 3 100r 1 17r 2 35r 1 17r 2 35r 1 43r 2 1 6r 2 27r 1  
117r 3 99r 1 17r 2 37r 1 16r 2 35r 1 42r 2 1 1r 2 1 3r 2 28r 1  
116r 3 97r 1 19r 2 38r 1 16r 2 36r 1 41r 2 4r 1 1r 2 28r 1 117r 3  
95r 1 20r 2 40r 1 15r 2 37r 1 40r 2 4r 1 1r 2 28r 1 80r 2 11r 1  
25r 3 93r 1 21r 2 40r 1 16r 2 38r 1 38r 2 4r 1 2 28r 1 79r 2  
16r 1 22r 3 94r 1 20r 2 40r 1 17r 2 36r 1 39r 2 3r 1 1r 2 28r 1  
77r 2 20r 1 20r 3 94r 1 20r 2 40r 1 18r 2 35r 1 39r 2 2r 1 2r 2  
27r 1 77r 2 22r 1 19r 3 95r 1 19r 2 40r 1 16r 2 34r 1 48r 2  
26r 1 77r 2 24r 1 18r 3 95r 1 20r 2 39r 1 16r 2 33r 1 49r 2  
26r 1 72r 2 1 2r 2 26r 1 17r 3 95r 1 20r 2 38r 1 16r 2 34r 1  
49r 2 25r 1 71r 2 4r 1 2 27r 1 17r 3 94r 1 18r 2 40r 1 16r 2  
34r 1 50r 2 23r 1 72r 2 34r 1 16r 3 95r 1 16r 2 41r 1 16r 2  
34r 1 50r 2 22r 1 73r 2 35r 1 15r 3 95r 1 15r 2 42r 1 16r 2  
33r 1 52r 2 19r 1 75r 2 35r 1 15r 3 95r 1 10r 2 2r 1 2 42r 1  
15r 2 1 2 27r 1 2 4r 1 54r 2 16r 1 77r 2 1r 1 2 32r 1 14r 3  
95r 1 9r 2 46r 1 17r 2 26r 1 3r 2 3r 1 56r 2 11r 1 83r 2 32r 1  
15r 3 94r 1 9r 2 45r 1 18r 2 25r 1 5r 2 1r 1 153r 2 33r 1 14r 3  
94r 1 9r 2 44r 1 19r 2 25r 1 107r 2 8r 1 44r 2 33r 1 14r 3 95r 1  
8r 2 43r 1 21r 2 25r 1 103r 2 14r 1 41r 2 33r 1 14r 3 95r 1  
11r 2 37r 1 25r 2 24r 1 101r 2 19r 1 39r 2 32r 1 14r 3 95r 1  
12r 2 35r 1 26r 2 24r 1 100r 2 21r 1 39r 2 31r 1 15r 3 95r 1  
11r 2 35r 1 27r 2 23r 1 99r 2 24r 1 34r 2 34r 1 15r 3 95r 1  
11r 2 35r 1 28r 2 22r 1 98r 2 26r 1 32r 2 35r 1 15r 3 95r 1  
12r 2 35r 1 27r 2 21r 1 93r 2 3r 1 2 28r 1 30r 2 36r 1 15r 3  
95r 1 12r 2 35r 1 28r 2 19r 1 93r 2 35r 1 29r 2 36r 1 16r 3

94r 1 12r 2 35r 1 30r 2 16r 1 94r 2 36r 1 27r 2 36r 1 17r 3  
94r 1 13r 2 34r 1 32r 2 12r 1 96r 2 37r 1 26r 2 36r 1 17r 3  
94r 1 13r 2 34r 1 35r 2 6r 1 100r 2 1r 1 2 33r 1 27r 2 34r 1  
18r 3 95r 1 13r 2 33r 1 146r 2 34r 1 26r 2 34r 1 18r 3 96r 1  
12r 2 33r 1 146r 2 34r 1 28r 2 31r 1 20r 3 94r 1 14r 2 31r 1  
147r 2 35r 1 29r 2 29r 1 20r 3 95r 1 14r 2 29r 1 148r 2 35r 1  
25r 2 32r 1 21r 3 95r 1 15r 2 28r 1 148r 2 35r 1 25r 2 30r 1  
23r 3 95r 1 16r 2 26r 1 150r 2 35r 1 23r 2 31r 1 24r 3 95r 1  
17r 2 22r 1 153r 2 34r 1 22r 2 33r 1 23r 3 95r 1 18r 2 20r 1  
153r 2 35r 1 17r 2 3r 1 2 33r 1 23r 3 95r 1 20r 2 16r 1 152r 2  
38r 1 17r 2 3r 1 2 33r 1 23r 3 95r 1 23r 2 11r 1 154r 2 38r 1  
17r 2 38r 1 23r 3 96r 1 27r 2 2r 1 113r 2 3r 1 39r 2 39r 1 17r 2  
39r 1 23r 3 95r 1 141r 2 11r 1 34r 2 39r 1 18r 2 38r 1 23r 3  
95r 1 139r 2 15r 1 32r 2 39r 1 22r 2 34r 1 24r 3 94r 1 130r 2  
1r 1 5r 2 18r 1 30r 2 38r 1 23r 2 34r 1 25r 3 94r 1 135r 2 21r 1  
30r 2 37r 1 23r 2 34r 1 26r 3 93r 1 129r 2 3r 1 1r 2 23r 1 29r 2  
35r 1 24r 2 33r 1 23r 3 1r 1 3 94r 1 129r 2 30r 1 29r 2 34r 1  
25r 2 32r 1 24r 3 95r 1 130r 2 31r 1 29r 2 32r 1 26r 2 32r 1  
22r 3 97r 1 131r 2 30r 1 27r 2 34r 1 27r 2 30r 1 21r 3 107r 1  
62r 2 8r 1 51r 2 31r 1 25r 2 35r 1 28r 2 29r 1 19r 3 111r 1  
57r 2 15r 1 47r 2 32r 1 23r 2 36r 1 28r 2 28r 1 19r 3 114r 1  
53r 2 19r 1 44r 2 33r 1 23r 2 36r 1 29r 2 26r 1 18r 3 119r 1  
48r 2 22r 1 43r 2 34r 1 22r 2 37r 1 30r 2 23r 1 18r 3 122r 1  
45r 2 25r 1 41r 2 34r 1 18r 2 1r 1 2 38r 1 31r 2 20r 1 19r 3  
125r 1 42r 2 27r 1 40r 2 34r 1 17r 2 42r 1 33r 2 17r 1 18r 3

131r 1 37r 2 29r 1 39r 2 34r 1 17r 2 41r 1 37r 2 12r 1 19r 3  
135r 1 29r 2 1r 1 2r 2 30r 1 38r 2 35r 1 16r 2 41r 1 41r 2 3r 1  
23r 3 138r 1 26r 2 4r 1 2 31r 1 38r 2 34r 1 17r 2 40r 1 68r 3  
142r 1 23r 2 38r 1 38r 2 33r 1 18r 2 1 1r 2 35r 1 68r 3 145r 1  
21r 2 38r 1 38r 2 33r 1 21r 2 35r 1 67r 3 147r 1 20r 2 39r 1  
37r 2 33r 1 22r 2 34r 1 65r 3 150r 1 23r 2 35r 1 37r 2 33r 1

- 
- 
- 

10r 2 19r 1 20r 3 1r 1 1r 3 46r 1 1r 3 300r 1 13r 2 18r 1 18r 3  
2r 1 3 48r 1 3 299r 1 1r 3 4r 1 10r 2 15r 1 17r 3 353r 1 1r 3  
8r 1 10r 2 12r 1 16r 3 2r 1 3 350r 1 3 12r 1 12r 2 6r 1 15r 3  
373r 1 10r 2 5r 1 14r 3 377r 1 27r 3 381r 1 23r 3 385r 1 19r 3  
382r 1 3 6r 1 14r 3 386r 1 3 1 3 4r 1 10r 3 386r 1 2r 3 1r 1  
3 4r 1 7r 3 401r 1 3r 3 404r 1 1r 3 404r 1 1r 3 405r 1 3  
45876r

c

c Cell Containing Lattice

c

997 0 -1111 fill = 996 imp:p 1 imp:e 1

c

c ++++++

c

c Surfaces

c

c ++++++

c

999 so 500 \$500cm universe sphere

c

c Box for Filling Universes

c

1111 rpp	0.000	203.0	0.000	204.0	0.000	30.2
2222 rpp	0.000	0.5	0.000	0.5	0.000	0.1
3333 rpp	0.000	0.39	0.000	0.39	0.000	0.09

c

c ++++++

c

c Materials

c

c ++++++

c

c Larvae

m1

1000	-0.0740	\$larvae
6000	-0.4837	

7000 -0.0485  
8000 -0.3938

c  
c Wall  
m2

1000 -0.136 \$Wall  
6000 -0.817  
8000 -0.047

c  
c Surrounding Air  
m3

7000 -0.755  
8000 -0.232  
18000 -0.013

c  
c ++++++

c  
c Source

c  
c ++++++

c  
mode p e  
sdef erg=0.01 par=2 eff=0.00001 X=d1 Z=d3 cel=d4  
si1 0.001 0.39  
sp1 0 1

si2 0.001 0.39  
sp2 0 1  
si3 0.001 0.09  
sp3 0 1  
si4 L (1<996<997) \$larvae  
sp4 1  
\*f8:e u=(1) \$larvae  
\*f18:e u=(2) \$wall  
e8 0 0.000001 6.0  
e18 0 0.000001 6.0  
PRDMP 3j 2 j  
nps 2000000